CrystEngComm

Accepted Manuscript

ROYAL SOCIETY OF CHEMISTRY

www.rsc.org/crystengcomm

Structural library of coordination polymers based on flexible linkers exploiting the role of linker coordination angle: synthesis, structural characterization and magnetic properties†

Bharat Kumar Tripuramallu, Paulami Manna and Samar K .Das*

School of Chemistry, University of Hyderabad, P.O. Central University,
Hyderabad- 500046, India.
E-mail: skdsc@uohyd.ernet.in; samar439@gmail.com
Fax: +91-40-2301-2460; Tel: +91-40-2301-1007

† Electronic supplementary information (ESI) available: Complete list of bond lengths and bond angles, $1/\chi_M$ *vs* *T* plots, powder X-ray diffraction patterns, TGA Curves and diffuse reflectance spectra and X-ray crystallographic data for compounds **1a**, **2a**, **3a**, **3b**, **4a** and **4b**; CCDC reference numbers 978685-978690. For ESI and crystallographic data in CIF or other electronic format see DOI:

Abstract

Herein we report six new coordination polymers $[Co(1,2-pda)(1,2-bix)]_n$ (**1a**), $[Co(hfipbb)(1,2-bix)]_n \cdot nH_2O$ (**2a**), $[Co(ADA)(1,2\text{-}bix)]_n$ (**3a**), $[Co(ADA)(1,3\text{-}bix)]_n \cdot nH_2O$ (**3b**), $[Co(1,4-pda)_2(2-pztz)]_2[Co(H_2O)_6] \cdot 2nH_2O$ (**4a**), $[Co_2(\mu\text{-}OH)(1,3-pda)(4-ptz)]_n$ (**4b**) based on the flexible carboxylate ligands 1,2−phenylenediaceticacid (1,2−H_2pda), 1,3−phenylenediaceticacid (1,3−H_2pda), 1,3-adamantanediacetic acid (H_2ADA) 4,4′-(hexa-fluoroisopropylidene)bis(benzoicacid) (H_2hfipbb) and secondary N-donor ligands 1,3−bis (imidazole-1-ylmethyl)-benzene (1,3−bix), 1,2−bis (imidazole-1-ylmethyl)-benzene (1,2−bix), 5-(4-Pyridyl) tetrazole (4−ptz) and 2-(2H-tetrazol-5-yl)pyrazine (2−pztz). All the compounds are characterized by single crystal X-ray diffraction analysis, IR spectroscopy, elemental analysis and bulk homogeneity by powder X-ray diffraction. A subtle relation between the position of the coordinating groups in the linker (known as linker coordination angle, LCA) with the dimensionality and topology of the final architectures of the title compounds has been discussed systematically by comparing with those of structurally related reported compounds $[Co(1,4-pda)(1,4-bix)]_n$ (**1b**), $[Co(hfipbb)(1,4-bix)_{0.5}]_n$ (**2b**) and $[Co_2(\mu\text{-}OH)(1,4\text{-}pda)(4\text{-}ptz)]_n \cdot nH_2O$ (**4c**). The compounds, studied in the present work, are classified into four different mixed linker classes, based on the skeleton geometry of the linker. Finally, the temperature dependent magnetic susceptibility measurements have been studied and the relevant zero-field splitting parameters have been determined.

Introduction

Because of enormous varieties of fascinating structural topologies and great potential applications as solid functional materials, metal organic frameworks (MOFs) and coordination polymers (CPs) have currently attracted considerable attention in recent years.[1] One of the most successful design strategies for constructing CPs is to take advantage of the versatility of several bridging ligands. Organic ligands with well-defined geometries may greatly influence the final structures of coordination polymers (CPs).[2] In case of designing the coordination polymers by using mixed linkers, the position of the coordinating groups on the linker often plays a major role in directing the dimensionality.[3] The general positions of the coordinating groups in the simple phenyl linker are ortho-, meta-, and para-bidentate modes. The angle between the positions of coordinating groups in the linker, which is known as linker coordination angle (LCA), varies according to geometry of the spacer; as a result, the overall coordination geometry of the concerned linker in the resulting CP alters, for example, bent, linear etc. Zhou and co-workers reported the application of mixture of bridging linkers with different LCAs in coordination-driven self assembly process.[4] The coordination networks, based on rigid ligands exploiting the LCAs, have extensively been studied due to their regular and well defined coordination modes.[5] In contrast, coordination polymers, constructed using flexible ligands are still limited, because of the unpredictable nature of such systems, because the flexible nature of spacers allows more number of degrees of freedom.[6]

Currently considerable efforts have been devoted to enriching the structural library of coordination networks, based on flexible ligands. The major parameters, to be considered in designing the ditopic flexible ligand based coordination networks, are the nature of the secondary ligand, coordination availability at the metal coordination sphere, length of the spacer and position of the coordinating groups. All these factors have tendency to modulate the conformations of the flexible ligands which is primarily responsible for the formation of higher dimensional structures. In ditopic flexible linkers, the geometrical orientation of two coordinating groups, associated with secondary linker, results in the construction of coordination networks of varying topologies that can exhibit unique functional properties. Cao and co-workers reported a series of coordination polymers based on the flexible ligands and used these compounds as functional materials for potential applications.[7] In our previous reports, we have discussed the factors affecting the conformational modulation of flexible ligands by exploring the role of secondary linker and metal ion.[8] Cao's group and we have demonstrated the conformation control of flexible ligand (H_2pda from *trans* to *cis*

conformation) by introducing a rigid auxiliary ligand, e.g., 4,4′-bipyridine / rigid tetrazole linker.[8,9] Shi and group reported a series of Zn(II) coordination polymer containing compounds from isomeric phenylenediacetic acid (1,4-, 1,3-, 1,2-H_2pda) and dipyridyl ligands.[10] The literature reports of the mixed linker coordination networks, based on flexible linkers exploiting the position of the coordinating groups in the linker, are very rare. We have been primarily working on coordination networks based on flexible linkers and reported our thoughts (in a conceptual manner) during analyzing the self-assembly processes of flexible linkers and transition metal ions, we have used in our laboratorty.[11]

This concept prompted us to study the influence of the linker coordination angles (LCAs) of various flexible ligands in designing coordination networks of versatile topologies. We have chosen diverse linkers, e.g., flexible phenylene diacetates,[12] bent flexible adamantane diacetic acid,[13] bent 4,4′-(hexa-fluoroisopropylidene)bis(benzoicacid),[14] flexible bisimidazolyl nitrogen donars,[15] and rigid tetrazoles[16] in exploring the library of coordination networks with possible varied linker coordination angles. We have described the design and synthesis of a new series of coordination polymer containing compounds $[Co(1,2{-}pda)(1,2{-}bix)]_n$ (**1a**), $[Co(hfipbb)(1,2{-}bix)]_n{\cdot}n H_2O$ (**2a**), $[Co(ADA)(1,2\text{-}bix)]_n$ (**3a**), $[Co(ADA)(1,3\text{-}bix)]_n{\cdot}nH_2O$ (**3b**), $[Co(2{-}pztz)(1,4{-}pda)_2]_2[Co(H_2O)_6]{\cdot}2nH_2O$ (**4a**) and $[Co_2(\mu\text{-}OH)(1,3{-}pda)(4{-}ptz)]_n$ (**4b**). In order to understand the affect of linker coordination angle (LCA), the above-mentioned compounds (present work) are compared with the three other compounds reported earlier by us,[8] namely $[Co(1,4{-}pda)(1,4{-}bix)]_n$ (**1b**) $[Co(hfipbb)(1,4{-}bix)_{0.5}]_n$ (**2b**) and $[Co_2(\mu{-}OH)(1,4{-}pda)(4{-}ptz)]_n{\cdot}n H_2O$ (**4c**). In the present study, the mixed coordination networks are broadly classified into four different classes based on the geometry of their skeleton, as (flexible, flexible), (bent, flexible), (bent flexible, flexible) and (rigid, flexible); the first term in the domain corresponds to the carboxylate linker and second term to the secondary N-donor linker. Additionally, the magnetic exchange interactions between the metal centers and single ion anisotropy of the compounds are characterized through variable temperature magnetic susceptibility measurements and relevant results have been described.

Experimental Section

Materials and methods

All the chemicals were received as reagent grade and used without any further purification. The ligands 1,4−bix, 1,3−bix, 1,2−bix, 4−ptz, 2−tzpz were prepared according to the literature procedures.[17] Elemental analyses were determined by FLASH EA series 1112 CHNS analyzer. Infrared spectra of solid samples were obtained as KBr pellets on a JASCO – 5300 FT – IR spectrophotometer. Powder X-ray diffraction patterns were recorded on a Bruker D8-Advance diffractometer using graphite monochromated $CuK_{\alpha 1}$ (1.5406 Å) and $K_{\alpha 2}$ (1.54439 Å) radiations. Magnetic susceptibilities were measured in the temperature range 2–300 K on a Quantum Design VSM-SQUID. All the compounds were synthesized in 23 mL Teflon-lined stainless vessels (Thermocon, India).

Synthesis of [Co(1,2−pda)(1,2−bix)]$_n$ (1a)

A mixture of $CoCl_2 \cdot 6H_2O$ (0.25 mmol, 59.5 mg), 1,2 - pda (0.25 mmol, 48.5 mg) and 1,2−bix (0.25 mmol, 60.0 mg) was dissolved in 10.0 mL of distilled water and the pH of the reaction mixture was adjusted to 6.35 by 0.5 M NaOH solution. Then the resulting mixture was stirred for 30 min and transferred to 23 mL Teflon-lined stainless vessel, sealed, and heated at 160°C for 72 h and then cooled to room temperature over 48 h to obtain red block crystals. Yield: 60.3% (based on Co). Anal. Calcd for $C_{24}H_{22}CoN_4O_4$ (M_r = 489.39): C, 58.90%; H, 4.53%; N, 11.44%. Found: C, 58.45%; H, 4.35%; N, 11.01%. IR (KBr pellet, cm^{-1}): 3140, 2997, 2916, 1695, 1572, 1520, 1369, 1265, 1226, 1024, 949, 852, 810, 748, 721, 657.

Synthesis of [Co(hfipbb)(1,2−bix)]$_n$·*n*H_2O (2a)

A mixture of $CoCl_2 \cdot 6H_2O$ (0.25 mmol, 59.5 mg), H_2hfipbb (0.25 mmol, 98.0 mg) and 1,2−bix (0.25 mmol, 60.0 mg) was dissolved in assorted solvent mixture of H_2O (10.0 mL) + DMF (1.0 mL) and stirred for 30 min. The pH of the reaction mixture adjusted to 6.10 by adding 5M NaOH solution and placed in a 23 mL Teflon-lined stainless steel autoclave, which was sealed and heated at 160 °C for 72 h. The autoclave was allowed to cool to room temperature for 48 h. Deep blue colored block-shaped crystals of compound **2a** were obtained in 65.5% yield (based on Co). Anal. Calcd for $C_{31}H_{22}N_4F_6O_5Co$ (M_r = 703.46): C, 52.93%; H, 3.15%; N, 7.96%. Found: C, 52.65%; H, 2.98%; N, 7.48%. IR (KBr pellet, cm^{-1}): 3516, 3138, 3015, 1699, 1612, 1556, 1518, 1462, 1244, 1170, 1091, 968, 949, 777, 717, 653.

Synthesis of {Co(ADA)(1,2−bix)}$_n$ (3a)

A mixture of $CoCl_2 \cdot 6H_2O$ (0.25 mmol, 59.5 mg), H_2ADA (0.25 mmol, 63.3 mg) and 1,2−bix (0.25 mmol, 72.5 mg) in H_2O:MeOH (10:1) was stirred for 30 min and sealed in a 25 mL

Teflon-lined stainless steel autoclave (pH = 7.00). The resulting reaction mixture was heated at 130°C for 4 days, and then slowly cooled to room temperature. Blue crystals of **3a** were obtained in 60.3% yield (based on Co). Anal. Calcd for $C_{28}H_{30}CoN_4O_4$ (M_r = 545.49): C, 61.65%; H, 5.54%; N, 10.27%. Found: C, 61.49%; H, 5.35%; N, 10.42%. IR (KBr pellet, cm^{-1}): 3408, 3128, 3101, 2962, 2904, 2838, 1672, 1572, 1528, 1446, 1402, 1254, 1101, 953, 750, 723, 673.

Synthesis of {Co(ada)(1,3−bix)}$_n$ (3b)

The ligand 1,2−bix was replaced by ligand 1,3−bix (0.25 mmol, 60.0 mg) and allowed to react with $CoCl_2 \cdot 6H_2O$ (0.25 mmol, 59.5 mg) and H_2ADA (0.25 mmol, 63.3 mg) to obtain the compound **3b** and the blue crystals were filtered off with 40% yield (based on Co). Anal. Calcd for $C_{28}H_{34}CoN_4O_5$ (M_r = 565.52): C, 59.47%; H, 6.060%; N, 9.907%. Found: C, 59.23%; H, 6.11%; N, 9.76%. IR (KBr pellet, cm^{-1}): 3452, 3397, 3150, 3095, 2838, 1649, 1545, 1523, 1446, 1419, 1358, 1232, 1150, 1112, 942, 816, 739, 657.

Synthesis of [Co(2−pztz)(1,4−pda)$_2$]$_2$[Co(H$_2$O)$_6$]·2*n*H$_2$O (4a)

A mixture of $CoCl_2 \cdot 6H_2O$ (0.50 mmol, 119.0 mg), 1,4-pda (0.25 mmol, 48.5 mg) and 2-pztz (0.25 mmol, 37 mg), dissolved in H_2O (10.0 mL), was stirred for 30 min and the pH of the reaction mixture was adjusted to 5.4 by adding 5M NaOH solution. The reaction mixture was placed in a 23 mL Teflon-lined stainless steel autoclave, sealed and heated at 130 °C for 96 h. The autoclave was allowed to cool to 30 °C for 48 h. Deep red block-shaped crystals of compound **4a** were obtained in 65.5% yield (based on Co). Anal. Calcd for $C_{30}H_{38}Co_3N_{12}O_{16}$ (M_r = 999.51): C, 36.05%; H, 3.83%; N, 16.81%. Found: C, 35.15%; H, 3.24%; N, 16.69%. IR (KBr pellet, cm^{-1}): 3362, 3026, 2926, 1684, 1616, 1574, 1523, 1410, 1253, 1170, 972, 935, 842, 746.

Synthesis of [Co$_2$(μ-OH)(1,3−pda)(4−ptz)]$_n$ (4b)

A mixture of $CoCl_2 \cdot 6H_2O$ (0.50 mmol, 119 mg), 1,3−pda (0.25 mmol, 48.5 mg) and 4−ptz (0.25 mmol, 36.65 mg) was dissolved in 10 mL distilled H_2O which was adjusted to pH = 4.20 with 5 M NaOH solution. The resulting reaction final mixture was sealed in a 23 mL Teflon−lined stainless steel autoclave and heated at 160 °C for 3 days. Dark red block-shaped crystals were obtained are filtered off and collected in 55.2% yield. Anal. Calcd for $C_{16}H_{12}Co_2N_5O_5$ (M_r = 472.17): C, 40.70%; H, 2.56%; N, 14.83%. Found: C, 40.15%; H, 2.02%; N, 14.09%. IR (KBr pellet, cm^{-1}): 3574, 1614, 1601, 1442, 1419, 1394, 1290, 1221, 974, 842, 760, 715, 630.

Single crystal X-ray structure determination of the compounds

Crystal data of the compounds **1a**, **3a**, **3b**, and **4b** were collected on Oxford Xcalibur Gemini Eos CCD diffractometer at 298 K using Mo-Kα radiation (λ = 0.7107 Å). Data reduction was performed using CrysAlisPro (version 1.171.33.55)[18a] and SHELXL-97 was used to refine the structures. The compounds **2a**, **4a** were mounted on a three circle Bruker SMART-APEX CCD area detector system under Mo-Kα (λ=0.71073 Å) graphite monochromated X-ray beam with crystal to detector distance 60mm, and a collimator of 0.5 mm. The scans were recorded with an ω scan width of 0.3º. Data reduction performed by SAINTPLUS.[18b] Intensities were corrected for absorption using SADABS.[18c] The structures were solved using SHELXS-97[18d] and full-matrix least-squares refinements were performed using SHELXL-97[18e]. All the non-hydrogen atoms were refined anisotropically. Hydrogen atoms on the C atoms were introduced on calculated positions and were included in the refinement riding on the irrespective parent atoms. Crystal data, structure refinement parameters for all the compounds are summarized in Table 1. And complete list of bond lengths and bond angles are given in the section of supplementary information.

< Insert Table 1 here>

Results and discussion

Synthesis

In order to exploit the role of linker coordination angles (LCAs) in the coordination polymers, based on flexible linkers, we have chosen the following linkers: phenylenediacetates, bis (imidazole-1-ylmethyl)-benzene, bent flexible carboxylate linker 1,3-adamantane diacetic acid, bent carboxylate linker H_2hfipbb and rigid tetrazoles. The title compounds were synthesized under hydrothermal conditions and the reaction procedures were optimized to obtain best yields. $CoCl_2 \cdot 6H_2O$ was taken as the metal source in the synthesis of the compounds due to its versatility in forming octahedral, square pyramidal and tetrahedral coordination geometries. The syntheses of the compounds were performed at 160 ºC for **1a**, **2a**, and 130°C for **3a, 3b, 4a** and **4b** in an aqueous medium.

Linker Coordination Angle (LCA)

In ditopic linkers, the coordination angle between the positions of two coordinating groups in a linker is called as a linker coordination angle. For a simple rigid phenyl linker, three different linker coordination angles (i.e. 60°, 120°, and 180°) are possible between the two coordinating groups. Different terminologies are used to represent position of the coordinating groups in the linker such as, ortho, meta, para and (1,4)-, (1,3)-, and (1,2)- etc.

In case of designing coordination architectures with mixed linkers, the LCAs of both the linkers should be considered in obtaining the desired topologies. The task becomes more difficulty in case of flexible ditopic linkers, as they have more number of degrees of freedom.

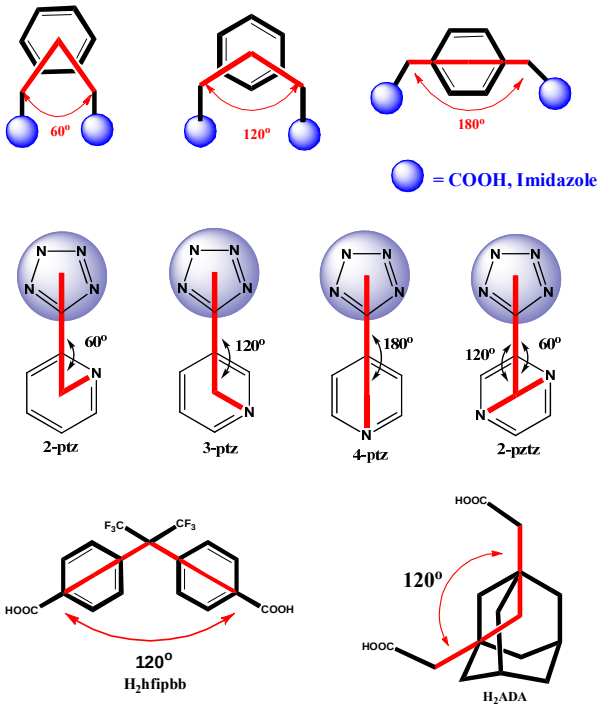

Scheme 1 Schematic representation of linker coordination angles of the flexible linkers employed in this study.

<Insert Table 2 here>

To reduce the complexity in measuring the linker coordination angle for flexible linkers, we have considered the angle between the two atoms of the linker where the coordination groups are connected, for example, the LCA of 1,3-pda is measured as the angle between two CH_2 groups of the acetate side chains with respect to the benzene ring, which is 120°. An important point to remember in quantifying the LCA is, it is different from the dihedral angle between the two coordinating groups and angle between two coordinating atoms. The LCAs of the ligands phenylenediacetates, bis (imidazole-1-ylmethyl)-benzene, bent carboxylate ligands H_2hfipbb and H_2ADA and rigid tetrazoles employed in this work are shown in the following scheme 1 and Table 2

In case of tetrazole ligands, as shown in the scheme 1, the LCA is measured between the tetrazole core ring and the position of the nitrogen atom in the pyridine ring. The LCAs mentioned in the above linkers are considered in their ideal geometry but in actual cases, these angles will vary to ± 10° based on the coordination consequences adopted by the linkers, e.g., $hfipbb^{2-}$ will have LCAs of 111°, 108° etc., ADA^{2-} has LCAs of 118° , 122° etc. In our previous article, we reported the factors affecting the conformational modulation

of flexible linkers in the self-assembly of coordination networks,[8] in which only few flexible linkers were used to explain these factors, but in order to rationalize this concept of flexibility in terms of coordination and dimensionality, an elaborated study is required. In view of this, in this article, we have demonstrated a library of coordination networks exploring the possible flexible linkers with rigid and bent secondary ligands.

Description of crystal structures

(Flexible, Flexible)

$[Co(1,2-pda)(1,2-bix)]_n$ (1a) and $[Co(1,4-pda)(1,4-bix)]_n$ (1b)

Compound **1b** is a 3D coordination polymer and the structural details are previously reported,[8] whereas, compound **1a** is 2D coordination polymer containing compound, that crystallizes in monoclinic space group $P2_1/c$. The asymmetric unit consists of one crystallographic independent Co(II) atom in a distorted tetrahedral geometry, one 1,2-pda^{2-} ligand and one 1,2-bix ligand. The distortion parameter τ_4 (= 0.87), calculated by the four-coordinate geometry index (τ_4={360°-(α+β)}/141, where α and β are the two largest angles of the tetrahedra), indicates slight distortion in tetrahedral geometry.[18f] The tetrahedral geometry around Co(II) atom is comprised of two oxygen atoms from two different 1,2-pda^{2-} ligands and two nitrogen atoms from two different 1,2-bix ligands (Fig. 1a). The carboxylate linker 1,2-pda^{2-} coordinates to the Co(II) center in μ_1-η_1,η_0 coordination mode on either sides and connects the adjacent Co(II) tetrahedra in a typical *trans* conformation with anticlinal torsion angle of 132.64° (viewed through N4-C24-C14-N2).The acetate side chains twisted with respect to phenyl ring through various extents *i.e.* 101.46° (through C4−C3−C2−C1) and 96.92° (through C7−C8−C9−C10). 1,2-pda^{2-} separates the two Co(II) centers with a distance of 8.512 Å to form a 1D metal-acid chain along the crystallographic *a* axis (Fig. 1b). These adjacent chains are connected to each other with the aid of 1,2−bix ligands along the *b* axis to form a 2D layer in the *ab* plane. 1,2−bix connects the Co(II) atoms of the adjacent chains in a typical *trans* conformation with antiperiplanar torsion angle of 151.22° (viewed through N4−C24−C14−N2) and creates of separation of 12.114 Å between the two metal centers in the adjacent chains. The dihedral angles between the imidazole ring planes and the least-squares plane of phenyl group are 74.01° and 77.50° respectively. The connectivity of the 1,2−bix to the metal acid chains result in the formation of 2D (4,4) connected sheets with dimensions of 12.114 × 8.512 $Å^2$ (Fig. 1c). The linker coordination angle between two imidazole rings in 1,2-bix is 60°, and due to less distance between two coordinating N atoms it has tendency to adopt cis conformation to form a molecular box, but

in this case, 1,2-bix adopts a trans conformation, thereby forming 2D layers. The presence of flexibility in the ligands, employed, result in the formation of wave like layer with crests and troughs at metal acid chains. These layers are stacked along the *c* axis in a ABAB fashion and the adjacent layers are tilted to ~ 7 Å and the alternate layers are arranged in back-to-back fashion as shown in Fig. 1d.

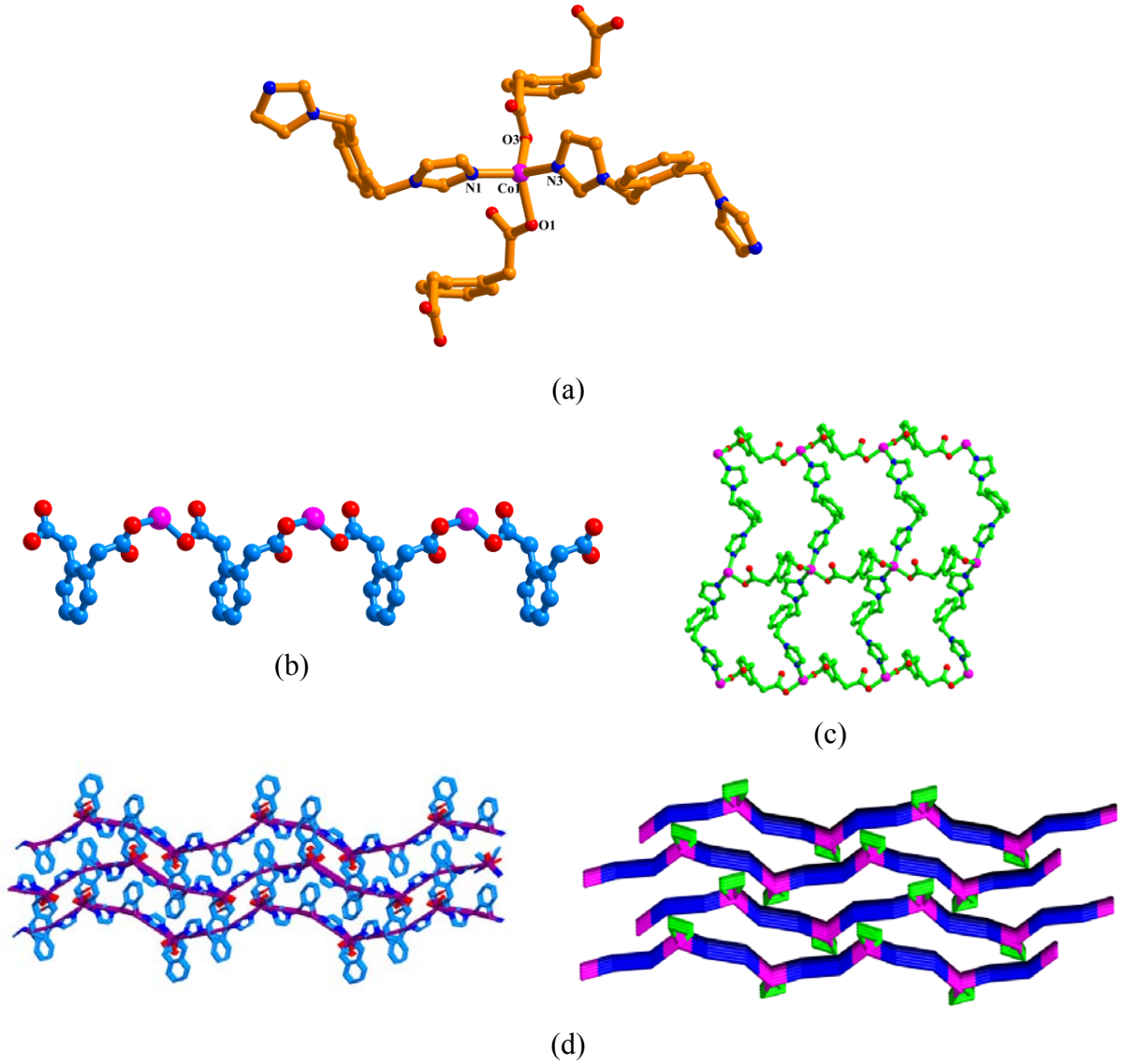

(a)

(b)

(c)

(d)

Fig. 1 (a) Coordination environment around the Co^{II} ion in **1a** with hydrogen atoms omitted for clarity. (b) 1D zig-zag chains formed due to Co-1,2-pda connectivity. (c) The overall 2D (4,4) connected sheets. (d) 3D stacking of 2D layers showing the tilting between two layers and its topological representation.

(Bent, Flexible)

$[Co(hfipbb)(1,2\text{-}bix)]_n \cdot nH_2O$ (2a) and $[Co(hfipbb)(1,4\text{-}bix)_{0.5}]_n$ (2b).

Compound **2a** is a 2D extended coordination polymer crystallizing in an orthorhombic space group *ccca*. Compound **2b** is a 3D layered pillared framework, as described in our previous report,[8] in which the 2D metal-hfipbb layers are pillared by the 1,4-bix linkers. The structural details and crystallographic details of **2b** are reported; herein we have discussed about compound **2a** only. The molecular diagram of **2b** consists of Co(II) atom in a slightly distorted tetrahedral $\{CoN_2O_4\}$ geometry with τ_4 of 0.93, constituted by the oxygen atoms from two different $hfipbb^{2-}$ units, and nitrogen atoms from two different 1,2-bix ligands and one lattice water molecule as shown in the Fig. 2a. The bond distances of Co–O and Co–N are in the range 1.957(3) – 2.023(3) Å and the bond angles around Co(II) centre are in the range 100.17° – 112.32°. The carboxylate groups in H_2hfipbb are completely deprotonated and each carboxylate group in $hfipbb^{2-}$ coordinates to the metal center in μ_1-η_1,η_0 coordination mode by creating a separation of 13.17 Å between two metal centers. The dihedral angle between the two benzene rings in the $hfipbb^{2-}$ anion is 74.77°, which is higher than that of 68.57° in the neutral H_2hfipbb ligand. The connectivity of $hfipbb^{2-}$ with the metal centers result in the formation of 1D metal acid zig-zag chains along the crystallographic *b* axis as shown in Fig. 1b. The metal-hfipbb systems are very well known in literature for the formation of paddle-wheel structures having open coordination site at the metal apical position, which is used to extend the dimensionality by the N-donor ligands.[14] Whereas, in the crystal structure of compound **1**, metal-hfipbb forms 1D chains; these chains are extended to form a 2D (4,4) connected sheets with the aid of 1,2-bix ligands.[15] 1,2-bix ligand connects the Co(II) atoms of the adjacent 1D chains in a typical *trans* conformation with antiperiplanar torsion angle of 151.84 ° (viewed through N2−C13−C13−N2) and creates a separation of 10.236 Å between the two adjacent chains. The overall connectivity of 1,2−bix ligands with the metal acid chains result in the formation of (4,4) corrugated sheets with dimensions of 13.177 × 10.236 $Å^2$ (Fig. 1c). The CF_3 groups, present on the $hfipbb^{2-}$, decorate the surface of the 2D layers. The corrugated nature of 2D layers allows the two layers to stack over each other to form a double layer with CF_3 groups above and below the double layer (Fig. 1d). These double layers are again stacked over each other resulting in the formation of two different types of cavities *i.e.,* fluorinated cavities formed due stacking of double layers and non fluorinated cavities due to stacking of monolayer's as shown in Fig. 1e. Two solvent molecules per cavity are present in the crystal structure and located exactly on the plane of the monolayer; as a result they are present in the nonflourinated cavity as shown in Fig. 2e.

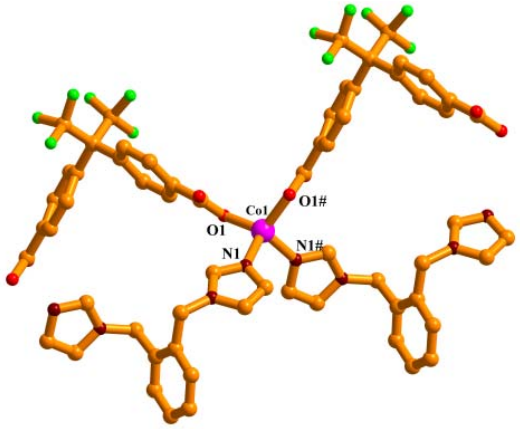

(a)

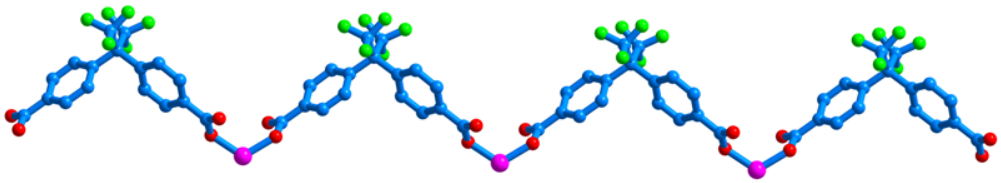

(b)

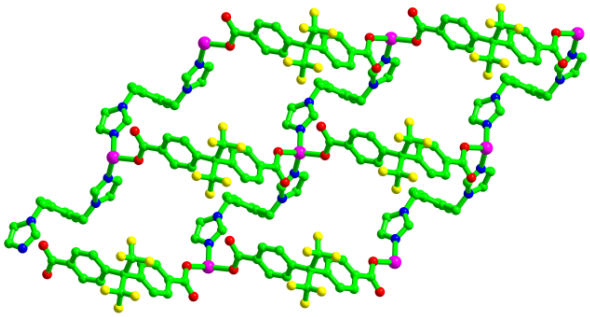

(c)

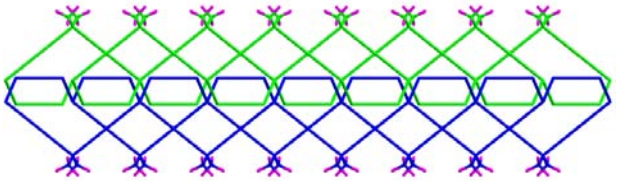

(d)

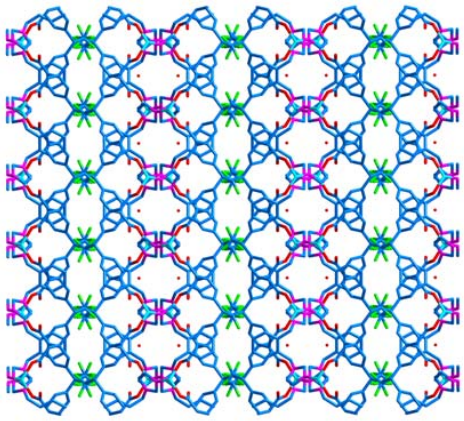

(e)

Fig. 2 (a) Molecular diagram of compound **2a** in atom labeling scheme at coordination sphere (b) 1D zig-zag chains formed due to Co-hfipbb connectivity. (c) 2D (4,4) connected topology viewing the square grid. (d) Stacking of two monolayers to form a double layer. (e) 3D stacking of double layers showing the two different types of cavities.

(Bent flexible, Flexible)

{Co(ADA)(1,2-bix)}$_n$ (3a)

The bent flexible linker H_2ADA reacts with Co(II)- 1,2-bix system, resulting in compound **3a**. Although compound **3a** forms a 2D grid-like layer structure, in this compound, Co(II) has slightly distorted tetrahedral geometry instead of octahedral geometry with a distortion parameter τ_4 of 0.78. Each Co(II) ion coordinates with two oxygen atoms from two different ADA^{2-} ligands and two N atoms from two 1,2-bix ligands (Fig. 3a). The bond distances of Co–O and Co–N are in the range 1.964(2) – 2.057(6) Å and the bond angles around Co(II) centre are in the range 95.75° – 106.30°. Both the carboxylate groups of the ADA^{2-} ligand adopts μ_1-η^1: η^0 coordination mode and each carboxylate group connects one Co(II) atom in mono-dentate fashion. The adjacent Co(II) atoms are connected by the ADA^{2-} ligand in *cis* conformation with torsion angle 10.55°(viewed through C1-C2-C14-C13) creating a Co···Co separation of 6.925 Å affording a 1D chain through the *b* axis. Interestingly, these chains have alternating right and left turns along the pitch of the ADA^{2-} resulting in the formation of a 1D zig-zag structure (Fig. 3b). The Co(II) centres in these chains are again connected by the 1,2-bix along the *c* axis creating a separation of 13.648 Å. 1,2-bix linker connects the Co(II) centers in typical cis conformation in which the dihedral angle between two imidazole rings is 30.39° and the dihedral angles between the imidazole rings and benzene rings are 75.31° and 75.21°. This associated connection of ADA^{2-} and 1,2-bix with Co(II) centre results in a 2D grid like layer structure along the crystallographic *bc* plane. Due to 1D zig-zag pattern of Co(II)- ADA^{2-} chains, the parallelograms formed by the connectivity of 1,2-bix ligands are resulted with two different dimensions (to be named as A and B) as shown in Fig. 3c. The parallelogram A has a larger area with dimensions of 18.265 X 11.612 $Å^2$ and B has a smaller area with dimensions of 20.016 X 8.234 Å. These parallelograms are arranged in alternate ABAB fashion in both the directions along the Co(II)- ADA^{2-} zig-zag chains and Co(II)-1,2-bix chains. These 2D layers are perfectly stacked on each other in eclipsed manner to arrange the parallelograms to form 1D channels (Fig. 3d). In addition, intermolecular hydrogen bonding were observed between C–H groups of ADA^{2-} linkers of one layer and carboxylate O atoms of ADA^{2-} linker of another layer through C8–H8•••O1 (with symmetry code 2 – x, 0.5 + y, 0.5 – z) with bond distance of 3.622 Å, along with some weak C–H•••N interactions between C–H groups of ADA^{2-} ligands and N atoms of imidazole rings. Hence, the two dimensional layers are connected to each other through C–H•••O and C–H•••N interactions to form a 3D supramolecular framework.

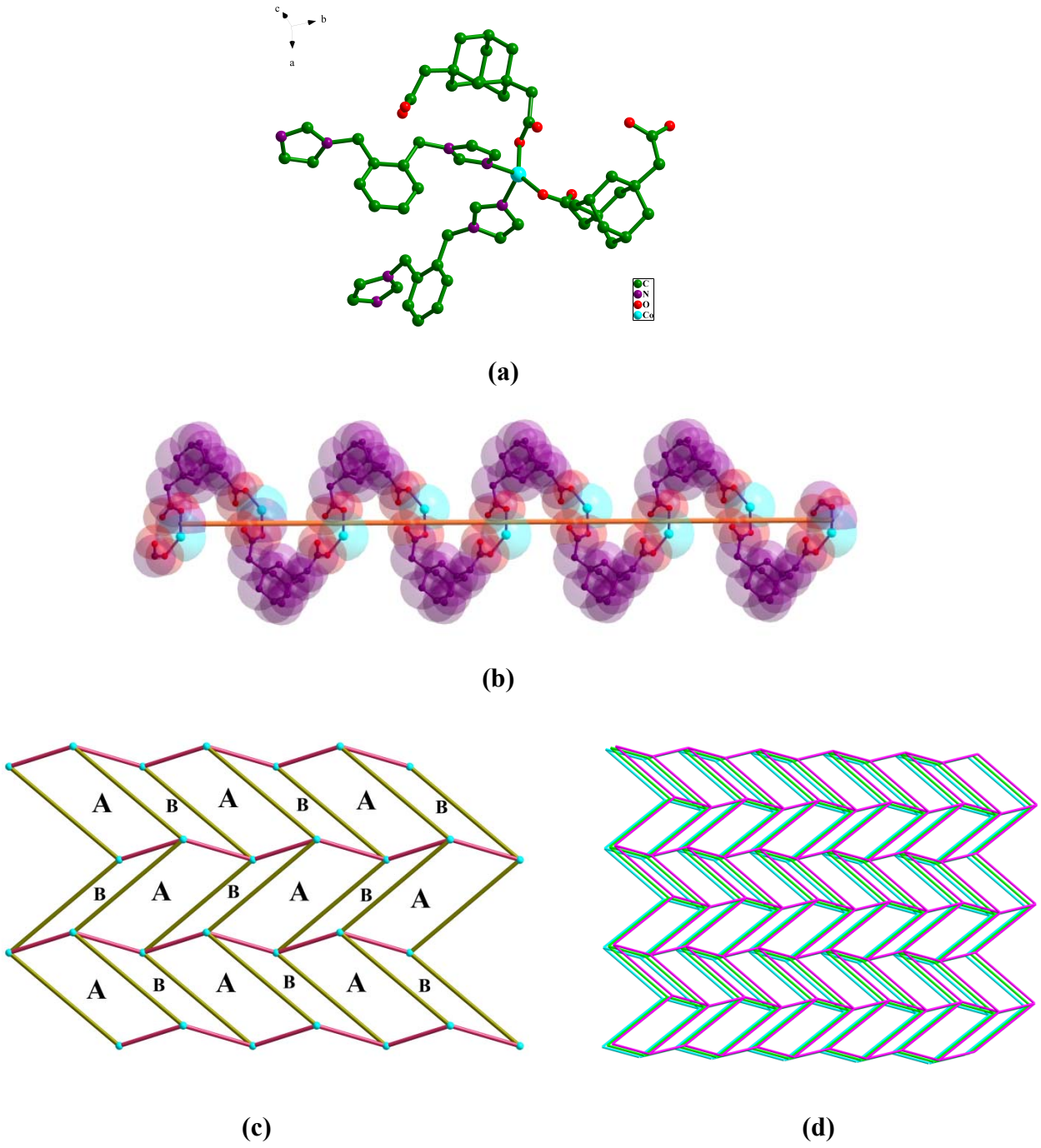

(a) **(b)** **(c)** **(d)**

Fig. 3 (a) The immediate coordination environment of Co(II) metal center in compound 3a (b) 1D zig-zag chains formed due to Co-ADA connectivity. (c) 2D (4,4) connected topology viewing the square grid with two different types of the parallelograms. (d) 3D eclipsed stacking of layers.

{Co(ADA)(1,3-bix)}$_n$•nH_2O (3b)

Compound **3b** is obtained by replacing the ligand 1,2-bix (LCA 60.0°) with 1,3-bix (LCA 120.0°). The molecular diagram consists of Co(II) ion in a distorted tetrahedral geometry with two O atoms from two different ADA^{2-} ligands, two N atoms from two different 1,3-bix

ligands and lattice water molecule (Fig. 4a). The distortion in the tetrahedral geometry around Co(II) centre, τ_4 is 0.73 which is considerably larger compared to τ_4 values, determined for compounds 1a, 2a and 3a. The Co(II)-O bond lengths are in the range of 2.052-2.158 Å, and Co(II)-N bond lengths are in the range of 2.062-2.082 Å, which are in good accordance with the literature. The bond angles around the Co(II) centre are in the range of 91.01-153.1° indicating the severe distortion in the tetrahedral geometry around the metal centre. In this compound, both the carboxylate groups of the acetate side chains in ADA^{2-} adopts μ_1-η^1: η^0 coordination mode and coordinate to the Co(II) centers by creating a separation of 10.19 Å. The acetate side chains in the ADA^{2-} linker adopt a *trans* conformation with torsion angle of 122.02° (viewed through C15-C16-C27-C28). The connectivity of ADA^{2-} with Co(II) centers result in the formation of 1D chains. In these Co(II)-ADA^{2-} chains, all the adamantane rings are located on the same side of the axis unlike zig-zag pattern observed in **3a** (Fig. 4b). These 1D chains are connected by the 1,3-bix linker by coordination of imidazole nitrogen atoms to Co(II) centers to form 2D sheets. The ligand 1,3-bix is a 1,3-positioned ligand with LCA of 120.0°, which exists in a trans conformation with torsion angle of 117.38 Å and creates a separation of 11.14 Å between two Co(II) centers of two adjacent Co(II)- ADA^{2-} chains. The overall connectivity of Co(II) centers with ADA^{2-} and 1,3-bix ligands results in the formation of 2D (4,4) connected corrugated sheets rather than a planar sheets (Fig. 4c). The flexibility, present in the ligand 1,3-bix, imparts the diagonal connectivity between two Co(II) centres of adjacent chains apart from linear connectivity; as a result, the 1D Co(II)-ADA^{2-} chains are arranged in a wavy ABAB fashion rather than planar AAAA fashion. One lattice water molecule per molecular formula unit is present in the crystal structure. These lattice water molecules are present exactly on the plane of the sheets and located in the void spaces created by (4,4) connectivity of metal centers. Interestingly, two lattice water molecules per parallelogram are arranged in alternative parallelograms as shown in the Fig. 4d. These lattice water molecules form strong hydrogen bonding interactions between the carboxylate oxygens of the same sheets forming a ten membered $R^4_4(10)$ rings inside the parallelograms alternatively. But no hydrogen bonding is observed between the adjacent sheets through lattice water molecules.

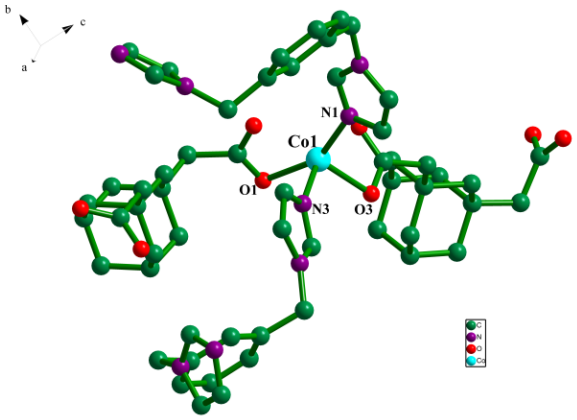

(a)

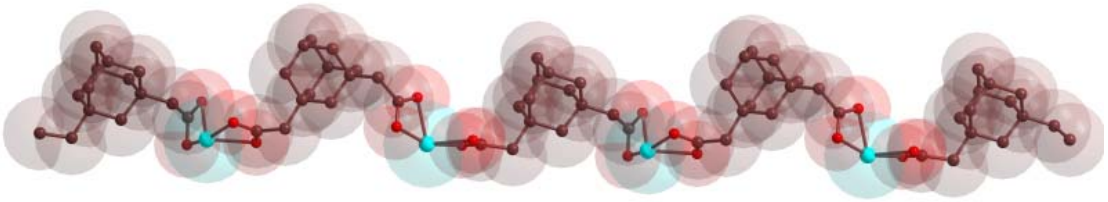

(b)

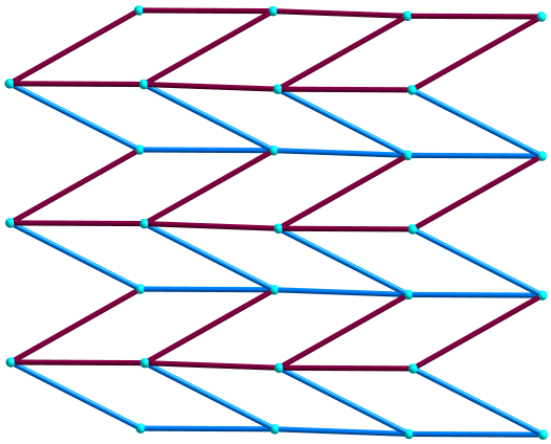

(c)

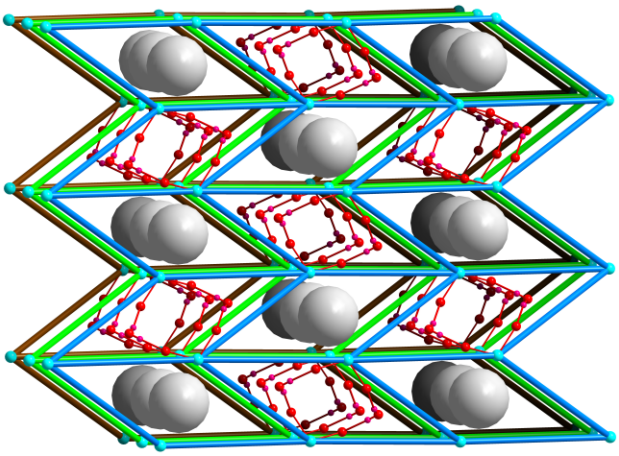

(d)

Fig. 4 (a) Molecular diagram of compound **3b** describing the coordination sphere (b) 1D zig-zag chains formed due to Co-ADA connectivity. (c) 2D (4,4) connected topology viewing the square grid.(d) Figure viewing the eclipsed stacking of monolayers containing $R^4_4(10)$ hydrogen bonding rings with the lattice water molecules in the channels and the empty channels .

(Flexible, Rigid)

[Co (1,4-pda)$_2$(2-pztz)]$_2$[Co(H$_2$O)$_6$]·2*n*H$_2$O (4a)

Compound **4a** is an 1D ion pair compound that crystallizes in triclinic space group *P-1*. The molecular diagram consists of 1D anionic chain $[Co(2-pztz)(1,4-pda)_2]^{2-}$ and lattice cationic $[Co(H_2O)_6]^{2+}$ units. The repeating unit in the 1D chain consists of two crystallographic independent Co(II) atoms in tbp geometry bridged by the two $2-pztz^{1-}$ ligands[21] and connected to four $1,4-pda^{2-}$ ligands (Fig. 5a). The tbp geometry of each Co(II) ion in the anionic chain is furnished by three nitrogen atoms from two different $2-pztz^{1-}$ ligands in the basal plane and two $1,4-pda^{2-}$ ligands in the apical positions. The pyrazine nitrogen atom N1 and tetrazole nitrogen atom N3 of 2-pztz coordinate to the Co(II) center in a chelating mode and these $Co(2-pztz)^{2+}$ are in turn connected by the nitrogen atom N4 (adjacent to nitrogen atom N3) of tetrazole ring to form a to form a six membered dimer ring with Co−Co separation of 4.179 Å. The overall connectivity of $2-pztz^{1-}$ ligands to metal centers result in the formation of the Co-dimer $\{Co_2(2-pztz)_2\}$ rings as shown in the Fig. 5b. The $2-pztz^{1-}$ in the crystal structure exhibits a μ_3 coordination mode (μ_2 from tetrazole ring and μ_1 from pyrazine ring) and the other nitrogen atom N2 in the pyrazine ring remains uncoordinated. The $\{Co_2(2-pztz)_2\}$ dimer connects to other dimer through two pairs of $1,4-pda^{2-}$ ligands in a typical *cis* conformation. Each $1,4-pda^{2-}$ coordinates to the metal center through μ_1 coordination mode and the acetate side chains in the skeleton are twisted with respect to each other through a synclinal torsion angle of 49.06 Å (viewed through C11−C12−C17−C18) indicating typical *cis* conformation. The presence of $1,4-pda^{2-}$ in the *cis* conformation result in the formation of $\{Co_2(1,4-pda)_2\}$ molecular loops as shown in Fig. 5c. Overall, the connectivity of these loops with the dimers result in the formation of 1D extended chain along the crystallographic *c* axis as shown in Fig. 5d. The hexa aqua cobalt(II) cations compensate the charge of the anionic chains staying as a lattice component. From the crystal packing diagram, $[Co(H_2O)_6]^{2+}$ cations are located between the two adjacent chains along the plane and nearly sandwiched between the two $\{Co_2(1,4-pda)_2\}$ loops along with the lattice water molecules (Fig. 5e). As anticipated, due to presence of lattice water molecules and coordinated water molecules in the hexa aqua cationic complex, strong hydrogen bonding were expected. The four coordinated water molecules in each $[Co(H_2O)_6]^{2+}$ cations are hydrogen bonded to carboxylate oxygen atoms of $1,4-pda^{2-}$ moieties of four anionic 1D chains and two lattice water molecules through O–H•••O interactions.

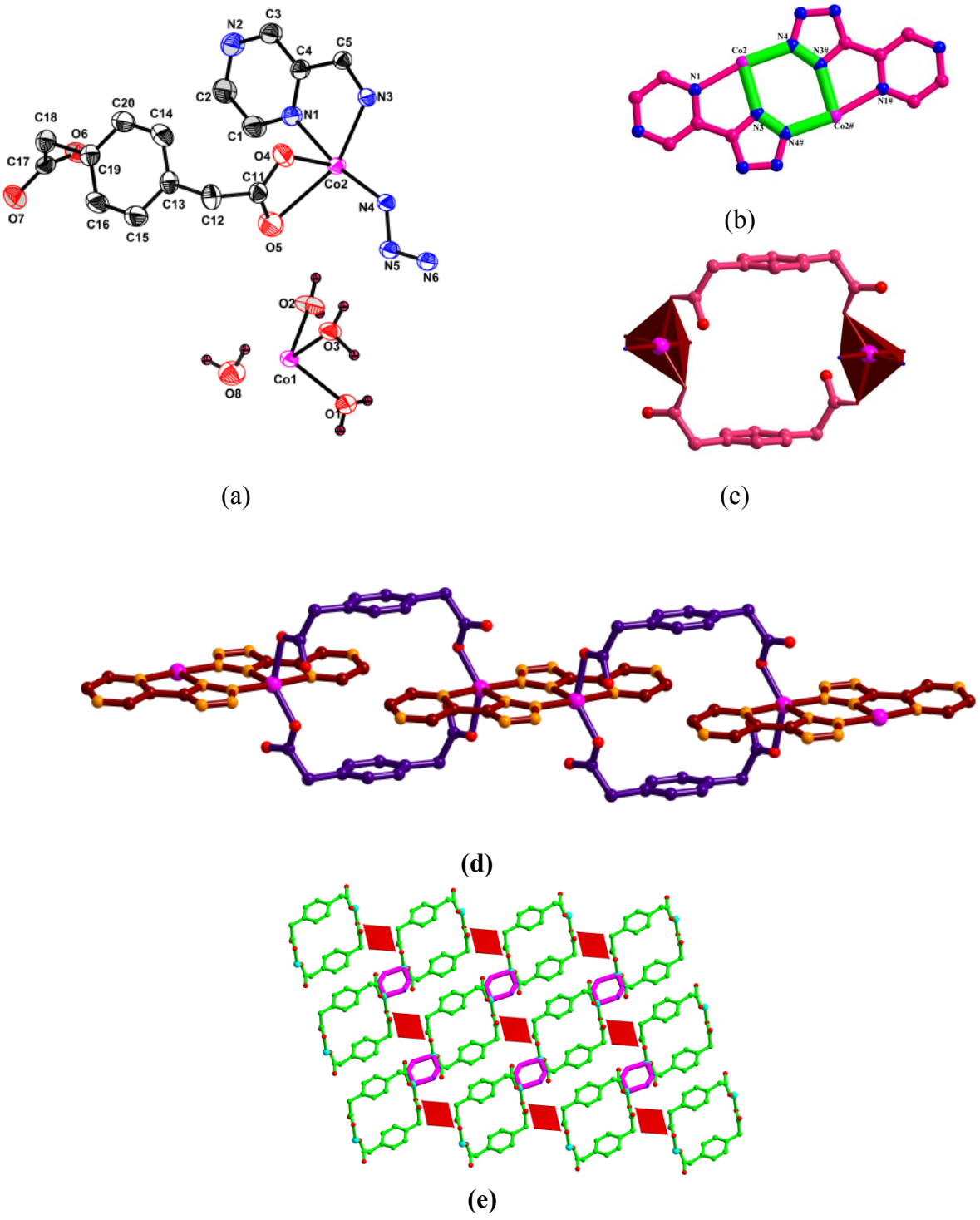

Fig. 5 (a) ORTEP view of the basic unit of **4a**. Hydrogen atoms of carbon atoms are been removed for clarity. Thermal ellipsoids are at the 30% probability level. (b) Co-dimer ring formed due to chelated connectivity of 2-pztz^{1-}(c) Molecular loop formed due to cis connectivity of the 1,4-pda^{2-} ligand.(d) 1D extended chain formed due to connectivity of 2-pztz and 1,4-pda ligands (e) 2D packing diagram illustrating the position of cationic species in the cavities.

$[Co_2(\mu\text{-}OH)(1,3\text{−}pda)(4\text{−}ptz)]_n$ (4b) and $[Co_2(\mu\text{-}OH)(1,4\text{−}pda)(4\text{−}ptz)]_n \cdot nH_2O$ (4c)

Both the compounds crystallize in monoclinic space group $P2_1/n$. The compounds **4b** & **4c** are isostructural except the carboxylate ligand 1,3−pda in **4b** is replaced by the 1,4-pda in **4c** and a lattice water molecule present in the compound **4c**, which is absent in compound **4b**. The structural description of the compound **4b** was elucidated in our previous report,[8] herein, we describe the structural description of **4c** and the structural consequences obtained by replacing 1,4−H_2pda with 1,3−H_2pda in terms of torsion angles and length of the ligand etc. The asymmetric unit of compound **4b** consists of two Co(II) atoms in tbp geometry connected by the μ_2-hydroxy group and one 1,3−pda^{2-} and 4−ptz^{1-} anion (Fig. 6a). Both the acetate groups in the 1,3−pda^{2-} anion adopts μ_2-η_1,η_1 coordination mode in a typical *cis* conformation with synclinal torsion angle of 29.84° (viewed through C8−C7−C9−C10), to form a metallo macrocycle, whereas the torsion angle exhibited by the acetate side chains of 1,4−pda^{2-} in compound **4b** is perfectly *cis* with synclinal torsion angle of 2.30 Å. The major structural changes, observed in the metallocycles formed due to *cis* connectivity of the carboxylate ligands *i.e.* 22-membered macrocycle with dimensions of 7.531 × 8.109 $Å^2$ was observed in case of 1,4-pda^{2-} whereas, 20-membered macrocycle with dimensions of 8.322 ×7.946 $Å^2$ was formed in case of 1,3−pda^{2-} associated compound. Also the benzene rings of pda^{2-} in the metallocycle formed in compound **4c** are faced parallel to each other due to 1,4−connectivity in the pda^{2-} ligand, but the benzene rings are not faced parallel to each other in compound **4b** due to 1,3−connectivity in the pda^{2-} ligand (Fig. 6b). The 20 membered macrocycle, formed in 4b extends its dimensionality with four another macrocycle through the bridging hydroxyl group (μ_2–OH) to form a 2D network (Fig. 6c). The co-ligand ptz in a μ_4 coordination mode (μ_3 from the tetrazole ring and μ_1 from the pyridine ring of the ptz) again connects this 2D network. The connectivity of tetrazole to Co(II) centres results in the formation of 1D chain in which the adjacent Co(II) ions are bridged by the nitrogen atoms of tetrazole ring and μ_2–OH groups. The connectivity of pda^{2-} in a *cis* conformation results in the formation of macrocycles which extends their dimensionality by bridging with μ_2–OH group and tetrazole ring to form 2D layers as shown in the Fig. 6d.

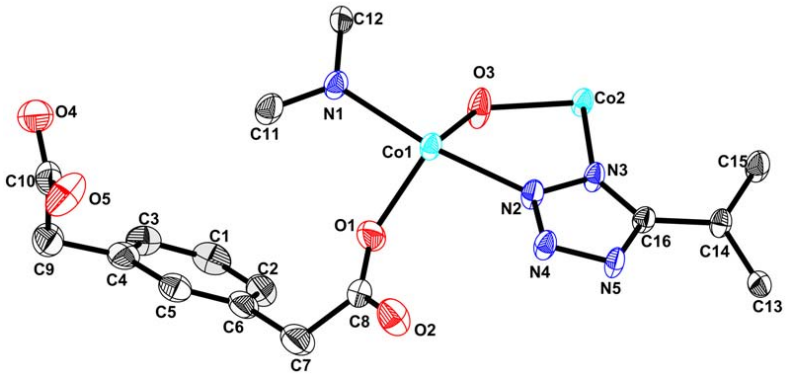

(a)

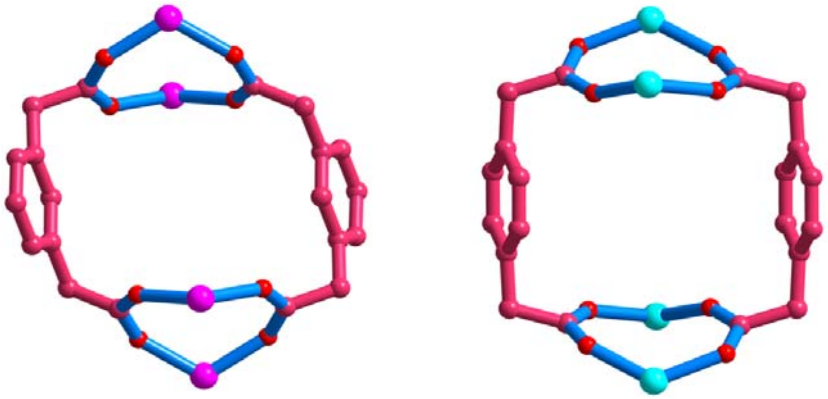

(b)

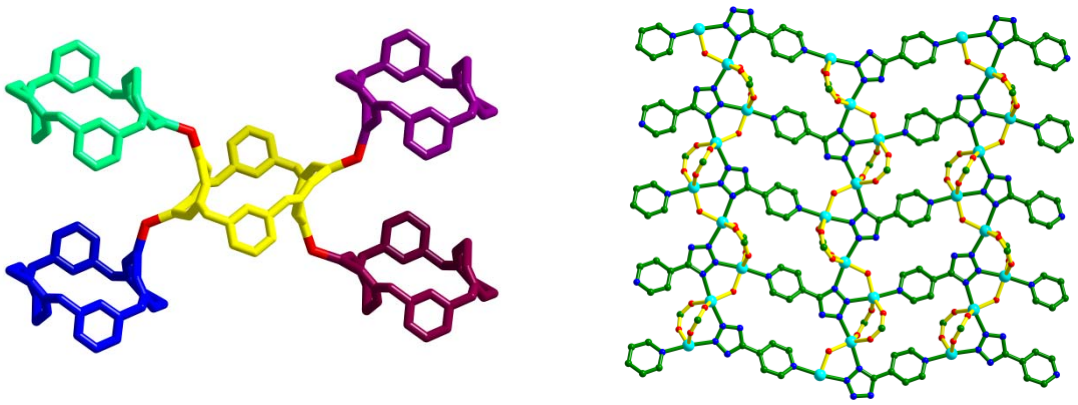

(c) **(d)**

Fig. 6 (a) ORTEP view of the basic unit of **4b**. Hydrogen atoms of carbon atoms are been removed for clarity. Thermal ellipsoids are at the 40% probability level. (b) Molecular box formed due to *cis* conformation of the pda^{2-} ligand (left for 1,3-pda^{2-} in 4b and right 1,4-pda^{2-} in 4c). (c) Four connectivity extension of molecular boxes through μ_2–OH group. (d) Overall 2D network of compound **4b** (phenylene rings of 1,3-pda^{2-} are omitted for clarity)**.**

Role of Linker Coordination Angle

Scheme 1 displays the possible LCAs of the phenylenediacetates, bis (imidazole-1-ylmethyl)-benzene, bent carboxylate ligand hfipbb^{2-}, bent flexible carboxylate linker ADA^{2-} and rigid tetrazoles. The combination of these linkers in constructing the mixed linker coordination networks would often lead to intriguing dimensionalities. The compounds, discussed, in this study are present under four different classes to demonstrate the rational affect of the linker coordination angle.

(Flexible, Flexible)

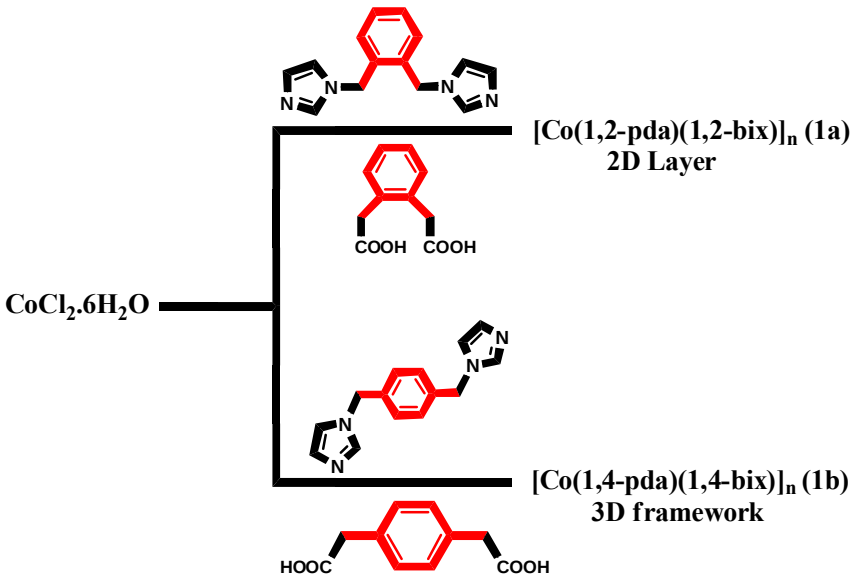

Scheme 2 Affect of dimensionality by changing the linker coordination angle of the isomeric bis (imidazole-1-ylmethyl)-benzene (bix) ligands and phenylene diacetate (pda) ligands.

In this section, two compounds **1a** and **1b** are synthesized with mixed (flexible, flexible) linkers system. As shown in the Scheme 2, the connectivity of 1,2−pda and 1,2−bix result in the formation of 2D layers in compound **1a** and the connectivity of 1,4−pda and 1,4−bix result in the formation of 3D framework in compound **1b**. In both the compounds, the Co(II) ion is present in the same {CoN_2O_4} tetrahedral geometry, but the linker coordination angle (LCA) changes the dimensionality of the compounds. In compound **1a**, the LCAs of both the ligands are 60° whereas, the LCAs of the ligands in compound **1b** are 180°. The difference in these LCA changes the length of the linker, resulting in changes in the annex of the linker. The linker with least LCAs generally creates the minimum separation between the metal polyhedra. The separation created by the 1,2−pda and 1,2−bix ligands in compound **1a** is

8.512 Å and 12.114 Å respectively, while the separation created by the 1,4−pda and 1,4−bix ligands in compound **1b** is 12.80 Å and 15.09 Å. Due to more length, the ligands protrude outside the layer to form a 3D framework, whereas, the short linkers connects to the metal centres in the same layer.

In both the compounds, the carboxylate ligands (1,2−pda and 1,4−pda) and N-donor secondary ligands (1,2−bix and 1,4−bix) adopt a *trans* conformation. The flexibility of the linkers is one among the reasons for the longer ones to protrude outside the 2D plane to form 3D structure (**1b**) and for shorter to hang about in the same plane (**1a**). Compounds **1a** and **1b** are mixed linker coordination networks in which both the linkers exhibit same LCA values *i.e.* either 60° and 60° in **1a** and 180° and 180° in **1b**. Perhaps in this system, the lower LCAs form 2D structures and higher LCAs form 3D structures and the linkers with mixed LCAs form either 2D or 3D only.

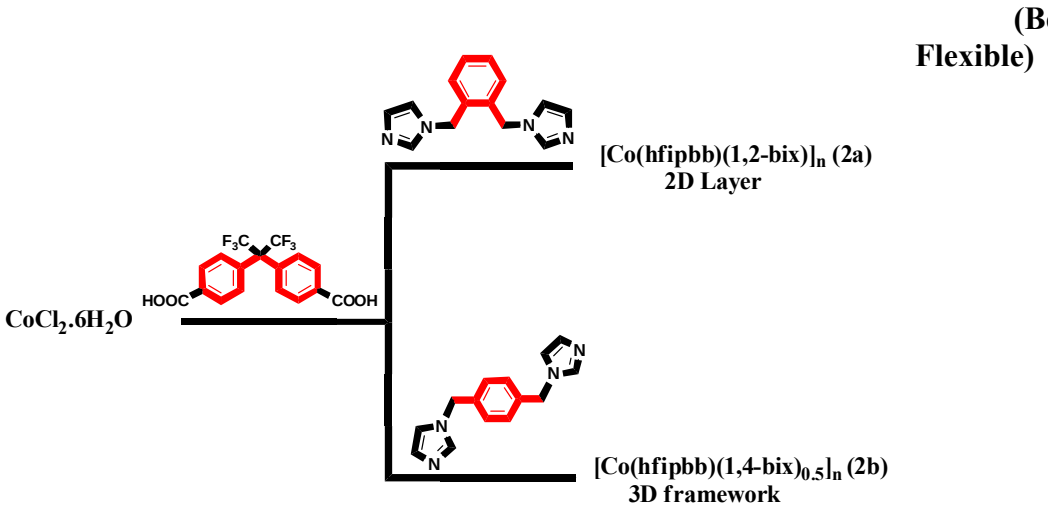

Scheme 3 Affect of dimensionality by changing the linker coordination angle of the isomeric bis (imidazole-1-ylmethyl)-benzene (bix) ligands with the metal-hfipbb system.

In this section, two compounds **2a**, **2b** with (Bent, flexible) mixed linker system are discussed. As shown in Scheme 3, the compounds **2a** and **2b** are constituted by the Co-hfipbb−(1,n)-bix (n=2,4) composition matrix. Compound **2a** is a 2D structure and **2b** is 3D layered-pillared framework. Both the compounds contain metal-hfipbb architectures which are extended by the bix linkers. In compound **2a**, metal-hfipbb forms 1D chains, which are connected by the 1,2−bix ligands to form 2D layers whereas, in **2b** metal-hfipbb forms a 2D helical double layers which are connected by the and 1,4−bix to form a 3D layered-pillared

framework. The linker coordination angles of 1,2−bix and 1,4−bix are 60° and 180°; as a result, the length of the ligands in the crystal structures are 7.75 Å and 11.21 Å respectively. In both the compounds, the bix linker adopts a *trans* conformation with variable torsion angles (151.84° for **2a**, and 180° for **2b**). The longer 1,4−bix favors the formation of metal-carboxylate paddlewheel layers in compound **2b**, since its length can separate these layers with definite distance to reduce the intermolecular repulsions. But the shorter 1,2−bix does not favor the formation of paddlewheels, as a result the metal-hfipbb forms 1D chains. In our previous report, the steric hindrance created secondary linker at coordination sphere for the formation of paddlewheels has been studied. From these two examples, it can be correlated that the formation of paddlewheels would be more favorable with the longer secondary linkers. In fact, this observation is in accordance with the other systems with longer linkers, e.g., 1,2-dpe bpy as found in the literature.

(Bent flexible, Flexible)

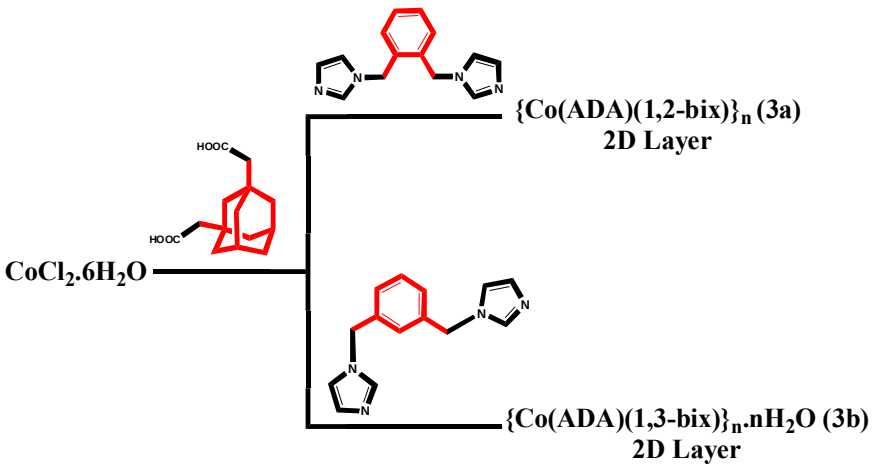

Scheme 4 Influence of LCA of secondary bix linker in modulating the topology of 2D layers in the isomeric bis (imidazole-1-ylmethyl)-benzene (bix) ligands with the metal-ADA system.

In this section, we tried to rationalize the effect of LCA with the (Bent flexible, flexible) mixed linker system. We have chosen 1,3-positioned adamantane diacetate linker with LCA 120° which also includes a flexibility in its geometry. The associated connectivity of ADA^{2-} with flexible bix linkers results in interesting topologies which differ from the expected ones. Both the compounds are 2D layers with 4,4 connected but the topology in both the cases are different from each other. In compound **3a**, 1,2-bix linker with LCA 60° exists in *cis* conformation and creates a large separation of 13.648 Å between two metal centers, but interestingly 1,3-bix linker with LCA 120° exists in trans conformation and creates a

separation of 11.146 Å between two Co(II) centers in **3b**. Usually 1,3-bix in *trans* conformation must creates a large separation than 1,2-bix in *cis* conformation, but a reverse fact is observed in case of compounds **3a** and **3b**. The main advantage of flexible linkers is that they can modulate their length according to the available coordination configurations by modulating their conformations. In this case, the coordination restrictions imposed by the ADA^{2-} in compounds **3a** and **3b** dictates the geometrical parameters of the bix linkers. In case of compound **3a**, ADA^{2-} forms a 1D zig-zag chain with left and right turns, whereas ADA^{2-} forms a 1D linear chain in **3b**. The connectivity of these 1D chains with bix linker forms different topologies; in case of 1,2-bix two different parallelograms are formed in the 2D layer and in case of 1,3-bix parallelograms with unique dimensions are formed in the 2D layer. This difference in the skeleton of 2D sheets can be correlated with the geometrical parameters exposed by the bix linkers.

(Flexible, Rigid)

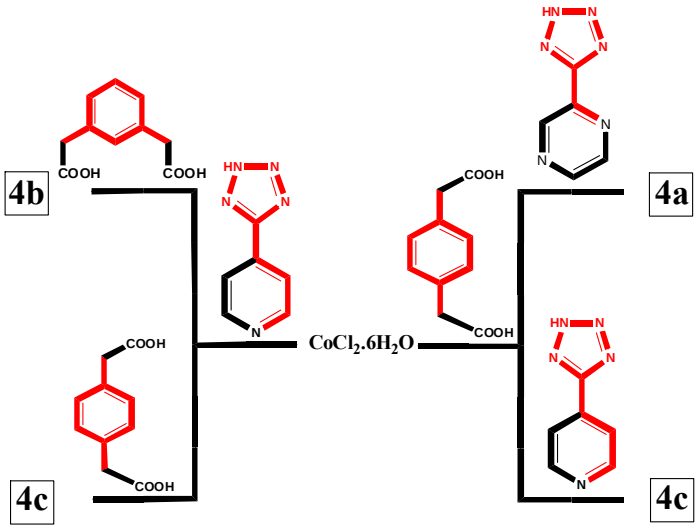

Scheme 5 Affect of dimensionality by changing the linker coordination angle of the isomeric phenylenediacetate ligands with different rigid tetrazole ligands.

In this section of compounds **4a**, **4b** and **4c**, (flexible, rigid) mixed linker system is considered. The important parameter in this discussion (for this type of mixed linker system) is when rigid secondary linker is used; the flexible primary linker always adopts *cis* conformation. As shown in the Scheme 5, both the compounds **4b** and **4c** are isostructural, even though the LCAs of the carboxylate linkers are 180° in **4b** and 120° in **4c**. In both these

compounds, the flexible carboxylate ligands adopt the *cis* conformation which primarily decreases the dimensionality. Usually *cis* conformations form low dimensional structures whereas *trans* conformations form high dimensional structures. In this scenario, the other factor *i.e.* LCA of secondary linker plays an important role in tuning the dimensionality. In compounds **4a** and **4b** the secondary linker is 4-ptz with LCA of 180°; as a result, both these compounds are 2D iso-structural compounds. Whereas in **4a**, when 1,4-pda adopts *cis* conformation, 1D chain is formed in this case, this is because the secondary ligand 2-tzpz has an LCA of 60°. In case of tetrazole linkers, the LCA was measured between the tetrazole ring and the position of nitrogen atom in the pyridine ring. When LCA is 60°, the skeleton of the tetrazole resembles with 2,2′-bipyridine and adopts chelated coordination mode thereby blocks the two coordination sites of Co(II) centers, which results in the lower dimensional compound **4a**; the cis conformation of 1,4-pda also favors the formation of 1D chain, as observed in case of **4a**. We tried to rationalize this effect with 2-ptz with LCA 60°, but we are unable to synthesize 2-ptz-1,4-pda assembled compound, so we have chosen 2-tzpz where it have two LCAs 60° and 120°, and fortunately in the crystal structure of **4a**, 2-tzpz utilizes only the LCA 60° which helps us to elucidate the affect of LCA. Overall, in the mixed linker (flexible, rigid) system, where flexible linker adopts *cis* conformation, the LCA of secondary linker decides the dimensionality of the final architectures. Also from these three examples, the (flexible, rigid) system always forms a 2D or 1D dimensional structures apart from higher 3D systems. The overall structural outcomes are tabulated in the Table 3.

<Insert Table 3 here>

XRPD and Thermogravimetric analysis

To ensure the phase purity of the compounds presented in the study powder X-ray diffraction of powder samples has been recorded**.** The diffraction patterns for the simulated data (calculated from single crystal data) are well matched with the observed data which proves the bulk homogeneity of the crystalline solids (see Section 3 of electronic supplementary information for the PXRD patterns). The experimental patterns have few un-indexed diffraction peaks and some are slightly broadened and shifted in comparison to those simulated patterns but still it can be regarded that the bulk as-synthesized materials represent compounds.

TGA plots were recorded under flowing N_2 for crystalline samples of the title compounds in the temperature range 40−1000 °C (see relevant plots in section-4, Supplementary information). Compound **1a** is stable up to 296°C and undergoes steep weight loss up to 402°C followed by continuous weight loss up to 1000 °C with a residual mass of

29.3 %. Compound **2a** losses one crystalline water with a weight loss of 2.63 % (theoretical weight loss 2.5 %) in the temperature regime of 40 °C to 115 °C and the network remains stable up to 295 °C. The dehydrated network undergoes sharp weight loss up to 455 °C and then undergoes continuous weight loss up to 1000 °C. The thermogravimetric curves of compound **3a** and **3b** follow the same path way, as both the compounds are stable up to 350 °C followed by decomposition of associated organic moieties in two steps at 475 °C and 535 °C with gradual weight loss up to 1000°C. Compound **4a** remains stable up to 100 °C and loses six coordinated water molecules of $[Co(H_2O)_6]^{2+}$ and two solvent water molecules in the temperature regime of 100 °C to 225 °C with weight loss of 14.9 % (theoretical 14.4 %); the dehydrated compound remains stable up to 306 °C and undergoes continuous weight loss up to 1000 °C. Compound **4b** is thermally stable up to 350 °C and undergoes a weight loss continuously in two steps at higher temperatures.

Electronic absorption properties

Solid state diffused reflectance spectra for all compounds were measured in the region 200–800 nm (the relevant spectra are presented in the section 5 of supplementary information). The absorption maxima at higher wave lengths 547 nm, 574 nm (for **1a**), 529 nm, 581 nm (for **2a**), 529 nm, 590 nm (for **3a**) 523 nm, 585 nm (for **3b**), 527 nm for **4a** and 522 nm for **4b** are tentatively assigned to d-d transitions in a d^7 Co(II) ion. The energy bands, observed at lower wave lengths in their electronic absorption spectra, are due to π−π* transitions from the phenyl rings which are in comparable with the transitions observed in the free ligands.

Magnetic Properties

Compound 2a

The magnetic properties of compound **2a**, as a plot of $\chi_M T$ *vs* T and χ_M *vs* T are shown in Fig. 7a. The $\chi_M T$ value at room temperature (300K) is 2.40 cm^3 K mol^{-1}, which is much higher than the expected value for isolated Co^{II} ion ($\chi_M T$ = 1.875 cm^3 K mol^{-1} for a S=3/2 ion). The $\chi_M T$ value decreasing gradually to 1.31 cm^3 K mol^{-1} at 2K. $1/\chi_M$ vs T follows the Curie Weiss law in the temperature range 2-300 K with negative Weiss constant θ= -5.23 K and C= 2.403 cm^3 K mol^{-1}. The higher value of $\chi_M T$ indicates the spin-orbit coupling of the tetrahedral Co(II) ion, which can be estimated by zero-field splitting (ZFS) effects of a single-ion of Co(II). The χ_M data in the temperature range 2 – 300 K was fitted by the following expressions for S=3/2 systems with dominant zero field splitting effects, D,[22] (eqs. 1–4):

$$\chi_{\parallel} = (Ng^2\beta^2/KT)[A/B] \qquad (1)$$

Where A=[1+ 9exp(–2*D/KT*)] and

B=[4(1+ exp(–2*D/KT*)]

$\chi_{\perp} = (Ng^2\beta^2/KT)[C/D]$ (2)

Where C = [4 + (3*K*T/D) (1– exp(–2*D/KT*)] and

D=[4(1+ exp(–2*D/KT*)]

$\chi_M' = [(\chi_{\parallel} + \chi_{\perp})/3]$ (3)

$\chi_M = \chi_M'/\{1 - \chi_M'(2zJ'/Ng^2\beta^2)\}$ (4)

The parameters ***N***, β and *K* have their normal meanings. The best fit obtained from 2–300 K with g= 2.27 (2) *D*= –6.07 (1) cm^{-1} and *zJ'*= 2.49 (6) with agreement factor of 1.82×10^{-4} . The value of D, calculated from the above expressions is in the range expected for tetrahedral metal center (i.e. D = –36 to +13 cm^{-1}).[22b] The D = –6.07 cm^{-1} indicates a 2D= 12.14 cm^{-1} splitting between the ground M_S= ±3/2 levels and the excited M_S= ±1/2 levels.

Compound 3b

The magnetic properties of compound **3b** possess roughly the same magnetic properties as compound **2a**. The plot of $\chi_M T$ *vs T* and χ_M *vs T* for compound **3b** in the temperature range 2 - 300K are shown in Fig. 7b. The $\chi_M T$ value at room temperature is 2.54 cm^3 K mol^{-1} which is higher than that of compound **3b** and it decreases slowly upto 2K (1.39 cm^3 K mol^{-1}). The Curie Weiss fitting reveals the value of θ= -7.4 K and C= 2.5 cm^3 K mol^{-1}, indicating the antiferromagnetic nature of the compound. The observed spin-orbit coupling was estimated by the zero-field splitting (ZFS) effects using the same equation as mentioned above. The best fitting of χ_M *vs T* data in the temperature range 2 – 300K gave g= 2.27 (2) *D*= –8.45 (1) cm^{-1} and *zJ'*= 3.62 (4). The higher D value indicates the larger splitting between the M_S= ±3/2 levels and M_S= ±1/2 levels compared to the compound **2a**.

Compound 4a

Both χ_M *vs T* and $\chi_M T$ *vs T* plots of the compound **4a** are presented in Fig. 7c. The room temperature $\chi_M T$ value of compound **4a** is 8.76 cm^3 K mol^{-1} which is much higher than the spin only value of 5.625 cm^3 K mol^{-1} for three Co(II) ions (*S*=3/2 and g=2) indicating the unquenched orbital contribution Co(II) ion. By lowering the temperature, the $\chi_M T$ value continuously decreases up to 2.41 cm^3 K mol^{-1} at 2K. The data follow the curie wises law with the Weiss constant θ= -20 K, agreeing the antiferromagnetic behavior of the compound, reflecting the plausible antiferromagnetic interaction between two Co(II) ions in the dimer through N atoms of the tetrazole ring. In compound **4a** two Co(II) ions are bridged by the nitrogen atoms of the tetrazole ring and the remaining Co(II) atom is in lattice position in

perfect octahedron. This factor makes difficult in analyzing the exchange phenomenon through the bridge. Because of the lack of a suitable model for such a system, fitting of the magnetic susceptibility and the relevant exchange parameters could not be estimated.

Compound 4b

The investigation of the magnetic study of compound 4b in the temperature range 2 -300 K reveals that the $\chi_M T$ value at the room temperature is 8.37 cm^3 K mol^{-1} which is much more higher than the spin only value (3.75 cm^3 K mol^{-1}) for two Co(II) ions (S=3/2 and g=2). As the temperature is lowered, there is a sharp decrease of $\chi_M T$ value continuously and reaches to a minimum value of 0.35 cm^3 K mol^{-1} at the 2K. The data of the χ_M *vs* T and $\chi_M T$ *vs* T plots (Fig. 7d) indicates the strong antiferromagnetic exchange between neighboring Co(II) metal ions. The strong antiferromagnetic exchange is also supported by the high Weiss constant θ= -160 K. As described in the crystal structure of the compound 4b, a 1D chain is formed by the connectivity of the Co(II) ions mixed bridged by double carboxylate bridges, hydroxo bridge, tetrazolate N_2 and tetrazolate N_3 bridge. The magnetostructure of the compound contains many pathways of the magnetic interaction; lack of the proper model for such system makes difficult to estimate the exchange parameters for this compound.

(a)

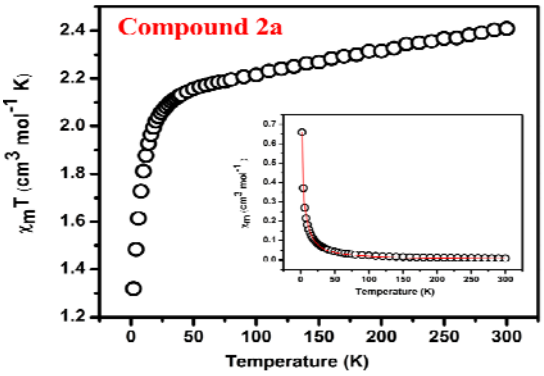

(b)

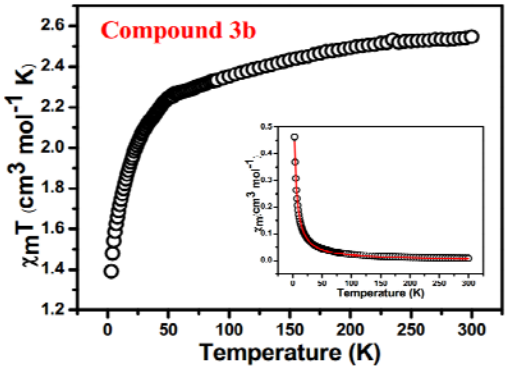

(c)

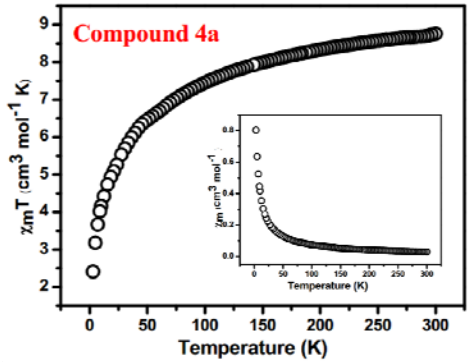

(d)

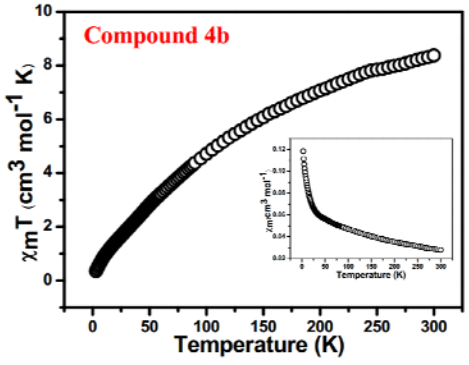

Fig.7 Plots of $\chi_M T$ *vs* *T* and χ_M *vs* *T* (inset) for the compounds **2a**, **3b**, **4a** and **4b** in the temperature range of 2–300K. The red line indicates the fitting using theoretical model (see text).

Conclusion

In designing coordination polymers based on the flexible linkers, several factors influence the self-assembly process; among those, the angle between the position of the coordinating groups *i.e.* linker coordination angle (LCA) is an important factor that alters the dimensionality and topology of the coordination networks. This concept has been discussed elaborately in this article taking a series of compounds, based on flexible linkers having intriguing skeletons. The self-assembly of (flexible, flexible) mixed linker system reveals the amendment of dimensionality according to length of the linker, dependent on LCA. The formation of Co-hfipbb matrix as 1D chain in **2a** and 2D interpenetrated double layer in **2b**, assisted by the secondary N–donor bix linkers having LCAs of 60° (for **2a**), and 180° (for **2b**) reveals the essential role of position of the coordinating groups on the linker. The associated connectivity of Co-ADA matrix with secondary N–donor bix linkers having LCAs of 60° (for **3a**), and 120° (for **3b**) results in formation of 2D layers with different topologies. Compounds **4a, 4b** and **4c** are coordination networks based on the {M-pda-tz} constituents in which the flexible carboxylates 1,4–pda in **4a** and **4c** and 1,3–pda in **4b** adopt a *cis* conformation which have same structural consequences on the dimensionality; in this situation, the LCA of the tetrazole directs the dimensionality in obtaining 2D structures in **4a** and **4b** with tetrazole of LCA 180° and 1D structure **4c** with tetrazole of LCA 60°. All the compounds, discussed in the study are series of examples to enrich the structural library of the coordination networks based on flexible linkers exploiting the role of linker coordination angle. Finally the temperature dependent magnetic susceptibility measurements divulge the zero-field splitting parameter of compounds **2a** and **3b** and the antiferromagnetic exchange interactions between the metal centers in **4a** and **4b**.

Acknowledgements

The authors thank the Department of Science and Technology, Government of India and CSIR, Government of India (Project No. 01(2556)/12/EMR-II) for financial support. The National X-ray Diffractometer facility at University of Hyderabad by the Department of Science and Technology, Government of India, is gratefully acknowledged. We are grateful

to UGC, New Delhi, for providing infrastructure facility at University of Hyderabad under UPE grant. BKT and PM thank CSIR, India for their fellowships.

Supporting Information Available: Crystallographic data in CIF format, PXRD patterns, Curie Weiss fitting plots, selected bond distances and angles in PDF format.

References

[1] (a) S. R. Halper, L. Do, J. R. Stork and S. M. Cohen, *J. Am. Chem. Soc*, 2006, **128**, 15255. (b) S. Hasegawa, S. Horike, R. Matsuda, S. Furukawa, K. Mochizuki, Y. Kinoshita and S. Kitagawa, *J. Am. Chem. Soc*, 2007, **129**, 2607. (c) S. Kitagawa and R. Matsuda, Coord. *Chem. Rev*, 2007, **251**, 2490. (d) O. M. Yaghi, M. O'Keeffe, N. W. Ockwig, H. K. Chae, M. Eddaoudi and J. Kim, *Nature,* 2003, **423**, 705. (e) F. Luo, J. M. Zheng and S. R. Batten, *Chem. Commun*, 2007, 3744.

[2] (a) R. Kitura, K. Fujimoto, S. Noro, M. Kondo and S. Kitagawo, *Angew. Chem. Int. Ed*, 2002, **41**, 133. (b) D. M. Shin, I. S. Lee and Y. K. Chung, *Inorg. Chem*, 2003, **42**, 8838. (c) P. Ayappan, O. R. Evans, Y. Cui, K. A. Wheeler and W. B. Lin, *Inorg. Chem*, 2002, **41**, 4978. (d) M. Dinca and J. R. Long, *J. Am. Chem. Soc*, 2005, **127**, 9376. (d) B. Bhattacharya, R. Dey , P. Pachfule, R. Banerjee , and D. Ghoshal *Cryst. Growth Des*, 2013, **13**, 731. (e) D. Ghoshal, G. Mostafa, T. K. Maji, E. Zangrando, T.-H. Lu, J. Ribas and N. R. Chaudhuri *New J. Chem.***,** 2004, **28**, 1204.

[3] (a) A. Schaate, S. Klingelhofer, P. Behrens and M. Wiebcke, *Cryst. Growth Des.*, 2008, **8**, 3200. (b) Y. Liu, Y. Qi, Y. Y. Lv, Y. X. Che and J. M. Zheng, *Cryst. Growth Des*, 2009, **9**, 4797. (c) Z. X. Li, T. L. Hu, H. Ma, Y. F. Zeng, C. J. Li, M. L. Tong and X. H. Bu, *Cryst. Growth Des*, 2010, **10**, 1138. (d) J. Yang, J. F. Ma, S. R. Battern and Z. M. Su, *Chem. Commun*, 2008, 2223.

[4] J.-R. Li and H.-C. Zhou, *Angew. Chem. Int. Ed,* 2009, **48**, 8465.

[5] a) A. J. Blake, N. R. Champness, S. S. M. Chung, W. S. Li and M. Schro¨ der, *Chem. Commun*, 1997, 1005. (b) M. Maekawa, H. Konaka, Y. Suenaga, T. K. Sowa and M. Munakata, *Dalton Trans*. 2000, 4160. (c) H. C. Wu, P. Thanasekaran, C. H. Tsai, J. Y. Wu, S. M. Huang, Y. S. Wen And K. L. Lu, *Inorg. Chem*, 2006, **45**, 295. (d) B. Y. Cho, D. Min and S. W. Lee, *Cryst. Growth Des*, 2006**, 6**, 342.

[6] (a) A. J. Blake, N. R. Brooks, N. R. Champness, M. Crew, A. Deveson, D. Fenske, D. H. Gregory, L. R. Hanton, P. Hubberstey and M. Schroder, *Chem. Commun*, 2001, 1432. (b) S. Sanda, S. Parshamoni , A. Adhikary and S. Konar *Cryst. Growth Des*.

2013, **13**, 5442 (c) S. Sanda ,S. Parshamoni and S. Konar, Inorg. Chem., 2013, **52**, 12866.

[7] (a) G. Li, J. Lu, X. Li, H. Yang and R. Cao, *CrystEngComm*, 2010, **12**, 3780. (b) T. F. Liu, J. Lu, X. Lin and R. Cao, *Chem. Commun*, 2010, **46**, 8439. (c) X. Li, X. Weng, R. Tang, Y. Lin, Z. Ke, W. Zhou and R. Cao, *Cryst. Growth Des*, 2010, **10**, 3228. (d) Z.-J. Lin, Y.-B. Huang, T.-F. Liu, X.-Y. Li, and R. Cao *Inorg. Chem*., 2013, **52**, 3127. (e) Z.-J. Lin , L.-W. Han, D.-S. Wu,Y.-B. Huang and R. Cao *Cryst. Growth Des.*, 2013, **13**, 255;(f) Z.-J. Lin, T.-F. Liu, Y.-B. Huang, J. Lü, R. Cao *Chem.-Eur. J*., 2012, **18**, 7896; (g) Z.-J. Lin, T.-F. Liu, X.-L. Zhao, J. Lü, and R. Cao *Cryst. Growth Des*., 2011, **11**, 4284

[8] B. K. Tripuramallu, P. Manna, S. N. Reddy and S. K. Das, *Cryst. Growth Des*, 2012, **12**, 777.

[9] T. Liu, J. Lu, L. Shi, Z. Guo and R. Cao, *CrystEngComm*, 2009, 11, 583.

[10] G. P. Yang, Y. Y. Wang, W. H. Zhang, A. Y. Fu, R. T. Liu, E. Lermontava and Q. Z. Shi, *CrystEngComm*, 2010, 12, 1509.

[11] (a) P. Manna, B. K. Tripuramallu, S. K. Das, *Cryst. Growth Des.*, 2012, ***12***, 4607. (b) B. K. Tripuramallu, S. Mukherjee, S. K. Das, *Cryst. Growth Des.*, 2013, **13**, 2426. (c) P. Manna, B. K. Tripuramallu, S. K. Das, *Cryst. Growth Des.*, dx.doi.org/10.1021/cg401502f.

[12] (a) L. Pan, K. M. Adams, H. E. Hernandez, X. Wang, C. Zheng, Y. Hattori and K. Kaneko, *J. Am .Chem. Soc.*, 2003, **125**, 3062. (b) O. Fabelo, L. C. Delgado, J. Pasan, F. S. Delgado, F. Lloret, J. Cano, M. Julve and C. R. Perez, *Inorg. Chem.*, 2009, 48, 11342. (c) C. Carpanese, S. Ferlay, N. Kyritsakas, M. Henry and M. W. Hosseini, *Chem. Commun.*, 2009, 6786.

[13] (a) J. C. Jin, Y. Y. Wang, P. Liu, R. T. Liu, C. Ren and Q. Z. Shi, *Cryst. Growth Des.*, 2010, **10**, 2019. (b) J. C. Jin, Y. Y. Wang, W. H. Zhang, A. S. Lermontov, E. Kh. Lermontova and Q. Z. Shi, *Dalton Trans*, 2009, 10181. (c) W. H. Zhang, Y. Y. Wang, E. Kh. Lermonntova, G. P. Yang, B. Liu, J. C. Jin, Z. Dong and Q. Z. Shi, *Cryst. Growth Des.*, 2010, **10**, 76.

[14] (a) H-L Jiang and Q. Xu *CrystEngComm*, 2010,**12**, 3815. (b) L. Han, Y. Zhou, W.-N Zhao, X. Li and Y.-X Liang *Cryst. Growth Des.,* 2009, **9** 660

[15] (a) I. Imaz, D. Maspoch, C. R. Blanco, J. M. P. Falcon, J. Campo and D. R. Molina, *Angew. Chem. Int. Ed*, 2008, **47**, 1857. (b) J. Yang, J. F. Ma, S. R. Batten and Z. M.

Su, *Chem.Commun*, 2008, 2233. (c) M. Sathiyendiran, J. Y. Wu, M. Velayudham, G. H. Lee, S. M. Peng and K. L. Lu, *Chem. Commun*, 2009, 3795.

[16] (a) B. K. Tripuramallu, R. Kishore and S. K. Das, *Inorg. Chim Acta*, 2011, **368**, 132. (b) P. Lin, W. Clegg, R. W. Harrington and R. A. Henderson, *Dalton trans,* 2005, 2388. (c) H. Zhao, Z. R. Qu, H. Y. Ye and R. G. Xiong, *Chem. Soc. Rev*, 2008, **37**, 84.

[17] (a) P. K. Dhal and F. H. Arnold, *Macromolecules*, 1992, **25,** 7051 (b) W. Ouellette, H. Liu, C. J. O'Connor and J. Zubieta, *Inorg. Chem*, 2009, **48**, 4655.

[18] (a) CrysAlis CCD and CrysAlis RED, Ver. 1.171.33.55; Oxford Diffraction Ltd: Yarnton, Oxfordshire, UK, 2008 (b) *SAINT: Software for the CCD Detector System*; Bruker Analytical X-ray Systems, Inc.: Madison, WI, **1998** (c) SADABS: Program for Absorption Correction; G. M. Sheldrick University of Gottingen: Gottingen, Germany, 1997. (d) SHELXS-97: Program for Structure Solution; G. M. Sheldrick, University of Gottingen: Gottingen, Germany, 1997. (e) SHELXL-97: Program for Crystal Structure Analysis; G. M. Sheldrick University of Gottingen: Gottingen, Germany, 1997. (f) L. Yang, D. R. Powell and R. P. Houser *Dalton Trans.*, 2007, 955.

[19] (a) L. Han, Y. Zhao, W. N. Zhao, X. Li and Y. X. Liang, *Cryst. Growth Des*, 2009, **9**, 660. (b) P. Pachfule, C. Dey, T. Panda and R. Banarjee, *CrystEngComm,* 2010, 12, 1600. (c) C. C. Ji, L. Qin, Y. Z. Li, Z. J. Guo and H. G. Zheng, *Cryst. Growth Des*, 2011, **11**, 480.

[20] (a) J. Yang, J.-F. Ma, S. R. Batten, S. W. Ng and Y.-Y. Liu, *CrystEngComm*, 2011, **13**, 5296. (b) H.-J. Lee, P.-Y. Cheng, C.-Y. Chen, J.-S. Shen, D. Nandi and H. M. Lee, *CrystEngComm*, 2011, **13**, 4814.

[21] (a) K. Darling, W. Ouellette, A. Prosvirin, S. Freund, K. R. Dunbar and J. Zubieta, *Cryst. Growth Des*, 2012, ***12***, 2662. (b) Z. Li, M. Li, X. –P. Zhou, T. Wu, D. Li and S. W. Ng, *Cryst. Growth Des*, 2007, ***7***, 1992.

[22] (a) S. R.Marshall, A. L. Rheingold, L. N. Dawe, W. W. Shum, C. Kitamura and J. S. Miller *Inorg. Chem.,* 2002*,* **41**, 3599. (b) M. W. Makinen, L. C. Kuo, M. B. Yim, G. B. Wells, J. M. Fukuyama, and J. E. Kim, *J. Am. Chem. Soc*. 1985, **107**, 5245.

Table 1 Crystal data and structural refinement parameters for compounds

	1a	2a	3a
Empirical formula	$C_{24}H_{22}CoN_4O_4$	$C_{31}H_{22}N_4F_6O_5Co$	$C_{28}H_{30}CoN_4O_4$
Formula weight	489.39	703.46	545.49
T(K) / λ(Å)	298(2), 0.71073	298(2), 0.71073	298(2), 0.71073
Crystal system	monoclinic	Orthorhombic	Monoclinic
Space group	*P2₁/c*	*Ccca*	P2(1)/c
a (Å)	8.5118(7)	13.177(8)	11.5867(3)
b (Å)	22.703(2)	15.668(8)	12.6968(4)
c (Å)	11.3906(8)	18.950 (16)	17.5141(5)
α (°)	90.00	90.00	90.00
β (°)	105.401(7)	90.00	96.216(3)
γ (°)	90.00	90.00	90.00
Volume (Å^3)	2122.1(3)	5977(5)	2561.42(13)
Z, ρ_{calcd} (g cm^{-3})	4, 1.532	8, 1.563	4, 1.415
μ (mm^{-1}), F(000)	0.850 /1012	0.660/2856	0.712/1140
goodness-of-fit on F^2	1.034	1.248	1.056
R1/ wR2 [I > 2σ (I)]	0.0535 / 0.0934	0.0687/0.1377	0.0398/ 0.1043
R1/ wR2 (all data)	0.0875 /0.1061	0.0867/0.1440	0.0529/0.1123
Largest diff peak/hole(e Å^{-3})	0.401 /–0.313	0.618/–0.307	0.627/-0.227

	3b	4a	4b
Empirical formula	$C_{28}H_{34}CoN_4O_5$	$C_{30}H_{38}Co_3N_{12}O_{16}$	$C_{16}H_{13}N_5O_5Co_2$
Formula weight	565.52	999.51	473.17
T(K)/ λ(Å)	298(2), 0.71073	298(2), 0.71073	298(2), 0.71073
Crystal system	Monoclinic	triclinic	monoclinic
Space group	P2(1)/n	*P-1*	*P2₁/n*
a (Å)	13.1976(9)	9.3717(8)	8.9732(4)
b (Å)	10.4914(7)	10.1843(9)	20.4712(9)
c (Å)	20.3760(15)	11.7377(11)	10.4084(5)
α (°)	90.00	112.9560(10)	90.00
β (°)	108.808(8)	106.240(2)	102.998(5)
γ (°)	90.00	90.6960(10)	90.00
Volume (Å^3)	2670.6(3)	967.32(15)	1862.95(15)
Z, ρ_{calcd} (g cm^{-3})	4, 1.407	1, 1.716	4, 1.687
μ (mm^{-1}), F(000)	0.688, 1188	1.360, 511	1.819, 948
goodness-of-fit on F^2	1.024	1.027	1.109
R1/ wR2 [I > 2σ (I)]	0.0440/0.1027	0.0322/ 0.0767	0.0448/ 0.1063
R1/ wR2 (all data)	0.0653/ 0.1166	0.0385/0.0802	0.0565/0.1120
Largest diff peak/hole (e Å^{-3})	0.422/ -0.376	0.357/ –0.229	0.879/ –0.302

Table 2 Linker coordination angles of various linkers employed in this work (see scheme 1)

Linker name	1,4-	1,3-	1,2-
Flexible			
pda	1,4−pda=180° (Linear)	1,3−pda =120° (Bent)	1,2−pda =60° (Chelated)
bix	1,4−bix =180° (Linear)	1,3−bix =120° (Bent)	1,2−bix =60° (Chelated)
H_2ADA	120° (Bent flexible)		
Rigid			
ptz	4−ptz =180° (Linear)	3−ptz=120° (Bent)	2−ptz =60° (Chelated) 2−pztz =60°,120° (Chelated, Bent)
H_2hfipbb	120° (Bent)		

Table 3 The structural outcomes of all the compounds presented in this study

Compound	LCA (Acid, N-Donor)	Mixed Linker Type*	Dimensionality
1a	180, 180	F,F	3D
1b	60,60	F,F	2D
2a	120,180	B,F	3D
2b	120,60	B,F	2D
3a	120,60	BF,R	2D
3b	120,120	BF,R	2D
4a	180,60	F,R	1D
4b	120,180	F,R	2D
4c	180,180	F,R	2D

* F= flexible, B= Bent, BF= Bent flexible, R= Rigid

TOC

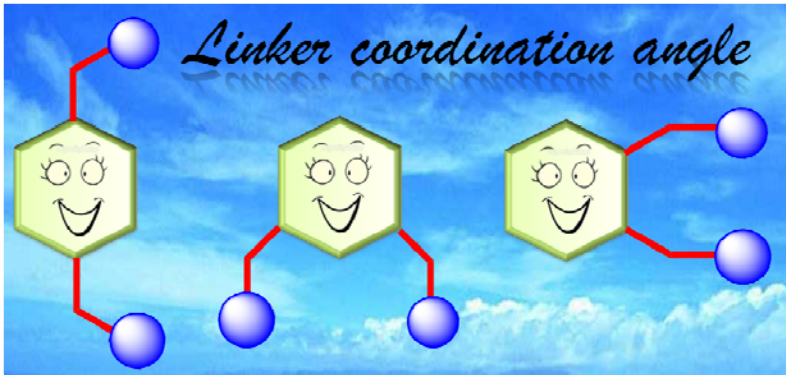

Text for TOC

The angles between the positions of the coordinating groups in the linker, termed as linker coordination angles, observed in the crystal structures of a new series of coordination polymers of flexible linkers, are correlated with the dimensionality and topology of the final architectures of the title compounds. The coordination polymers are additionally characterized by temperature dependent magnetism.